PHYSICAL REVIEW D VOLUME 3, NUMBER 9 1 MAY 1971

Hard-Meson Calculation of $K\pi$ Scattering*†

PAUL POND‡
Department of Physics, Northeastern University, Boston, Massachusetts 02115
(Received 11 September 1970)

The hard-meson $SU(3)\times SU(3)$ current-algebra four-point functions are applied to $K\pi$ scattering, using pole dominance of the σ commutators. The S- and P-wave scattering lengths and effective ranges are extracted. The hard-meson S-wave scattering lengths differ from the soft-pion Weinberg scattering lengths by only a few percent. Energy-dependent fits up to 1 GeV and above are made. All the available experimental data on the elastic and charge-exchange cross sections and phase shifts can be fitted using the parameter F_K/F_π.

I. INTRODUCTION

RECENTLY,[1] considerable effort has been devoted to the extraction of the $K\pi$ interaction from Kp experimental data. In spite of many uncertainties that still remain in these analyses, $K\pi$ cross sections and phase shifts up to roughly 1.5 GeV have become experimentally accessible. The purpose of the present paper is to calculate $K\pi$ scattering using a hard-meson current-algebra method and compare the result with all available experiment. The hard-pion techniques using $SU(2)\times SU(2)$ current algebra[2,3] have previously been successfully applied to $\pi\pi$ scattering, where excellent agreement with experiment up to 1 GeV was achieved.[4] The hard-pion method has also been extended to include strangeness-changing currents in order to analyze the K_{l3} decay.[5,6] More recently, the hard-meson method has been extended further, so that one can compute an arbitrary N-point function using the chiral $SU(3)\times SU(3)$ current algebra.[7]

We briefly review the physics involved in the hard-meson $SU(3)\times SU(3)$ current-algebra analysis. The basic assumptions here are (1) that the currents obey the equal-time commutation relations of Gell-Mann[8]; (2) that the vector currents are conserved (CVC), all the axial-vector currents are partially conserved (PCAC), and the strangeness-changing vector currents are partially conserved (PCVC) (these conditions are referred to collectively as PCC); (3) that the vacuum expectation values of the T-products of an arbitrary number of currents can be saturated by a few low-lying single-particle states; (4) smoothness of the particle vertex functions, which means that they may be approximated by a low-order polynomial in the momenta of the single particles involved. In the calculation of $K\pi$ scattering, which is an application of these techniques for a four-point function, we make one additional postulate, and that is the pole dominance of the σ commutator. As in the case of $\pi\pi$ current-algebra amplitudes, the $K\pi$ scattering requires the inclusion of a specific set of seagull terms along with the usual pole terms. Section II is devoted to a review of the general formalism for calculating four-point amplitudes. In Sec. III, S- and P-partial-wave amplitudes, S- and P-wave scattering lengths, and the S-wave effective range for $I=\frac{1}{2}$ and $I=\frac{3}{2}$ $K\pi$ scattering are computed. Section IV contains a comparison of the phase shifts and cross sections with the experimental data. A comparison with the Lovelace-Veneziano model is also given.

II. REVIEW OF HARD-MESON METHOD

The currents involved in the $K\pi$ calculation are governed by the chiral $SU(3)\times SU(3)$ current algebra (CCA) according to the equal-time commutation relations:

$$\delta(x^0-y^0)[V^0{}_a(x),V^\mu{}_b(y)] =i\epsilon_{abc}V^\mu{}_c(x)\delta^4(x-y)+c\text{-No. S.T.}, \quad (2.1a)$$

$$\delta(x^0-y^0)[V^0{}_a(x),A^\mu{}_b(y)] =i\epsilon_{abc}A^\mu{}_c\delta^4(x-y)+c\text{-No. S.T.}, \quad (2.1b)$$

$$\delta(x^0-y^0)[A^0{}_a(x),V^\mu{}_b(y)] =i\epsilon_{abc}A^\mu{}_c(x)\delta^4(x-y)+c\text{-No. S.T.}, \quad (2.1c)$$

* Supported in part by the National Science Foundation.
† Based on work contained in a PhD thesis submitted to Northeastern University.
‡ Present address: Department of Physics, Westfield College, University of London, London, N.W.3, England.
[1] For a comprehensive survey up to 1969 of the experimental and theoretical situation on $K\pi$ scattering, see *Proceedings of the Conference on $\pi\pi$ and $K\pi$ Interaction* (Argonne National Laboratory, Argonne, 1969).
[2] R. Arnowitt, M. H. Friedman, and P. Nath, Phys. Rev. Letters **19**, 1085 (1967); Phys. Rev. **174**, 1999 (1968); R. Arnowitt, M. H. Friedman, P. Nath, and R. Suitor, *ibid.* **175**, 1802 (1968).
[3] For work related to that of Ref. 2, see H. Schnitzer and S. Weinberg, Phys. Rev. **164**, 1828 (1967); I. S. Gerstein and H. J. Schnitzer, *ibid.* **170**, 1638 (1968); S. G. Brown and G. B. West, Phys. Rev. Letters **19**, 812 (1967); Phys. Rev. **168**, 1605 (1968); J. Schwinger, Phys. Letters **24B**, 473 (1967); J. J. Wess and B. Zumino, Phys. Rev. **163**, 1727 (1967); B. Lee and H. T. Nieh, *ibid.* **166**, 1507 (1968); T. Das, V. S. Mathur, and S. Okubo, Phys. Rev. Letters **19**, 859 (1967).
[4] R. Arnowitt, M. H. Friedman, P. Nath, and R. Suitor, Phys. Rev. Letters **20**, 475 (1968); Phys. Rev. **175**, 1820 (1968).
[5] R. Arnowitt, M. H. Friedman, and P. Nath, Nucl. Phys. **B10**, 578 (1969), and Northeastern University report, 1968 (unpublished).
[6] With additional assumptions but with similar techniques, the decay has also been examined by L. N. Chang and Y. C. Leung, Phys. Rev. Letters **21**, 122 (1968); I. S. Gerstein and H. J. Schnitzer, Phys. Rev. **175**, 1876 (1968); L. K. Pande, Phys. Rev. Letters **23**, 353 (1969); P. Auvil and N. Deshpande, Phys. Rev. **183**, 1463 (1969).
[7] R. Arnowitt, M. H. Friedman, P. Nath, and R. Suitor, Phys. Rev. D **3**, 594 (1971).
[8] M. Gell-Mann, Physics **1**, 63 (1964).

$$\delta(x^0-y^0)[A^0{}_a(x),A^\mu{}_b(y)] =i\epsilon_{abc}V^\mu{}_c(x)\delta^4(x-y)+c\text{-No. S.T.}, \quad (2.1\text{d})$$

$$\delta(x^0-y^0)[V^0{}_a(x),S^\mu{}_\alpha(y)] =-\tfrac{1}{2}(\tau_a)_{\alpha\beta}S^\mu{}_\beta(x)\delta^4(x-y)+c\text{-No. S.T.}, \quad (2.1\text{e})$$

$$\delta(x^0-y^0)[S^0{}_\alpha(x),V^\mu{}_a(y)] =\tfrac{1}{2}(\tau_a)_{\alpha\beta}S^\mu{}_\beta(x)\delta^4(x-y)+c\text{-No. S.T.}, \quad (2.1\text{f})$$

$$\delta(x^0-y^0)[V^0{}_a(x),C^\mu{}_\alpha(y)] =-\tfrac{1}{2}(\tau_a)_{\alpha\beta}C^\mu{}_\beta(x)\delta^4(x-y)+c\text{-No. S.T.}, \quad (2.1\text{g})$$

$$\delta(x^0-y^0)[C^0{}_\alpha(x),V^\mu{}_a(y)] =\tfrac{1}{2}(\tau_a)_{\alpha\beta}C^\mu{}_\beta(x)\delta^4(x-y)+c\text{-No. S.T.}, \quad (2.1\text{h})$$

$$\delta(x^0-y^0)[A^0{}_a(x),S^\mu{}_\alpha(y)] =-\tfrac{1}{2}(\tau_a)_{\alpha\beta}C^\mu{}_\beta(x)\delta^4(x-y)+c\text{-No. S.T.}, \quad (2.1\text{i})$$

$$\delta(x^0-y^0)[S^0{}_\alpha(x),A^\mu{}_a(y)] =\tfrac{1}{2}(\tau_a)_{\alpha\beta}C^\mu{}_\beta(x)\delta^4(x-y)+c\text{-No. S.T.}, \quad (2.1\text{j})$$

$$\delta(x^0-y^0)[A^0{}_a(x),C^\mu{}_\alpha(y)] =-\tfrac{1}{2}(\tau_a)_{\alpha\beta}S^\mu{}_\beta(x)\delta^4(x-y)+c\text{-No. S.T.}, \quad (2.1\text{k})$$

$$\delta(x^0-y^0)[C^0{}_\alpha(x),A^\mu{}_a(y)] =\tfrac{1}{2}(\tau_a)_{\alpha\beta}S^\mu{}_\beta(x)\delta^4(x-y)+c\text{-No. S.T.}, \quad (2.1\text{l})$$

$$\delta(x^0-y^0)[S^{\dagger 0}{}_\alpha(x),S^\mu{}_\beta(y)] =\tfrac{1}{2}\{(\tau_b)_{\beta\alpha}V^\mu{}_b(x)+\sqrt{3}\delta_{\beta\alpha}V^\mu{}_8(x)\}\delta^4(x-y) +c\text{-No. S.T.}, \quad (2.1\text{m})$$

$$\delta(x^0-y^0)[S^{\dagger 0}{}_\alpha(x),C^\mu{}_\beta(y)] =\tfrac{1}{2}\{(\tau_b)_{\beta\alpha}A^\mu{}_b(x)+\sqrt{3}\delta_{\beta\alpha}A^\mu{}_8(x)\}\delta^4(x-y) +c\text{-No. S.T.}, \quad (2.1\text{n})$$

$$\delta(x^0-y^0)[C^{\dagger 0}{}_\alpha(x),S^\mu{}_\beta(y)] =\tfrac{1}{2}\{(\tau_b)_{\beta\alpha}A^\mu{}_b(x)+\sqrt{3}\delta_{\beta\alpha}A^\mu{}_8(x)\}\delta^4(x-y) +c\text{-No. S.T.}, \quad (2.1\text{o})$$

$$\delta(x^0-y^0)[C^{\dagger 0}{}_\alpha(x),C^0{}_\beta(y)] =\tfrac{1}{2}\{(\tau_b)_{\beta\alpha}V^\mu{}_b(x)+\sqrt{3}\delta_{\beta\alpha}V^\mu{}_8(x)\}\delta^4(x-y) +c\text{-No. S.T.}, \quad (2.1\text{p})$$

where $V^\mu{}_a$ and $A^\mu{}_a$ ($a=1, 2, 3$) are the $SU(3)$ triplets of currents. $S^\mu{}_\alpha$ and $C^\mu{}_\alpha$ ($\alpha=1, 2$) are the strangeness-changing isodoublets of currents with $\alpha=1$ corresponding to $(4-i5)/\sqrt{2}$ and $\alpha=2$ corresponding to $(6-i7)/\sqrt{2}$, where 4, 5, 6, and 7 correspond to $SU(3)$ components. $V^\mu{}_8$ and $A^\mu{}_8$ are the eighth components of the $SU(3)$ vector and axial-vector currents, respectively. The τ's are the usual Pauli matrices and c-No. S.T. stands for c-number Schwinger terms. The isotriplet and isodoublet currents obey the partial conservation conditions (PCC)

$$\partial_\mu V^\mu{}_a=0\,, \qquad a=1, 2, 3 \quad (2.2)$$

$$\partial_\mu A^\mu{}_a=m_\pi{}^2F_\pi\pi_a\,, \quad a=1, 2, 3 \quad (2.3)$$

$$\partial_\mu C^\mu=m_K{}^2F_K K\,, \quad (2.4)$$

$$\partial_\mu S^\mu=m_\kappa{}^2F_\kappa \kappa\,, \quad (2.5)$$

where on the right-hand side in Eqs. (2.2)–(2.5) we have denoted the fields by their particle labels and F_π is the pion decay constant, m_π the pion mass, etc.

Arnowitt, Friedman, and Nath[2] (and other hard-meson workers[3]) couple the current-algebra conditions (2.1) and the PCC conditions with two dynamical assumptions to calculate T-products of currents. These assumptions are (1) single-particle saturation (the T-products of currents may be expressed in terms of matrix elements of currents between single-particle states), and (2) the resulting particle vertices may be approximated by a finite polynomial in the particle momentum. Assumption (1) implies the field-current identities[9]

$$V^\mu{}_a=g_\rho\rho^\mu{}_a\,, \quad (2.6\text{a})$$

$$A^\mu{}_a=g_A a^\mu{}_a+F_\pi\partial^\mu\pi_a\,, \quad (2.6\text{b})$$

$$C^\mu{}_\alpha=g_{KA}K_A{}^\mu{}_\alpha+F_K\partial^\mu K_\alpha\,, \quad (2.6\text{c})$$

$$S^\mu{}_\alpha=g_{K^*}K^{*\mu}{}_\alpha+F_\kappa\partial^\mu\kappa_\alpha\,. \quad (2.6\text{d})$$

In addition, the concept of single-meson saturation was shown to lead to a theorem which states that the T-product of an arbitrary number of currents can be computed from an effective Lagrangian which has the form

$$\mathfrak{L}=\mathfrak{L}_{(0)}+\mathfrak{L}_I\,, \quad (2.7)$$

where

$$\mathfrak{L}_I=g\mathfrak{L}_{(3)}+g^2\mathfrak{L}_{(4)}+g^3\mathfrak{L}_{(5)}+\cdots. \quad (2.8)$$

g is a coupling constant and $\mathfrak{L}_{(3)}$, $\mathfrak{L}_{(4)}$, etc., are cubic, quartic, etc., in the fields. Further, in calculating the T-product of N currents using $\mathfrak{L}_I$ one must only keep terms to order $(N-2)$ in the coupling constants. This is equivalent to calculating a T-product in the tree and seagull-diagram approximation. Hence to calculate $K\pi$ scattering, the effective Lagrangian need only be used to second-order perturbation theory.

For $K\pi$ scattering, the free-meson Lagrangian has the form

$$\mathfrak{L}_{(0)}=\mathfrak{L}_{(0)\pi}+\mathfrak{L}_{(0)K}+\mathfrak{L}_{(0)\sigma}+\mathfrak{L}_{(0)\kappa} +\mathfrak{L}_{(0)\rho}+\mathfrak{L}_{(0)A}+\mathfrak{L}_{(0)K^*}+\mathfrak{L}_{(0)K_A}\,, \quad (2.9)$$

where the free Lagrangians for the spin-zero mesons are

$$\mathfrak{L}_{(0)\pi}=-\pi^\mu{}_a(\partial_\mu\pi_a)+\tfrac{1}{2}(\pi^\mu{}_a\pi_{\mu a}-m_\pi{}^2\pi^2)\,, \quad (2.10\text{a})$$

$$\mathfrak{L}_{(0)K}=-[K_\mu{}^\dagger\partial^\mu K+\partial^\mu K^\dagger K_\mu] +K_\mu{}^\dagger K^\mu-m_K{}^2K^\dagger K\,, \quad (2.10\text{b})$$

$$\mathfrak{L}_{(0)\sigma}=-\sigma^\mu(\partial_\mu\sigma)+\tfrac{1}{2}(\sigma^\mu\sigma_\mu-m_\sigma{}^2\sigma^2)\,, \quad (2.10\text{c})$$

$$\mathfrak{L}_{(0)\kappa}=-[\kappa_\mu{}^\dagger\partial^\mu\kappa+\partial^\mu\kappa^\dagger\kappa_\mu]+\kappa_\mu{}^\dagger\kappa^\mu-m_\kappa{}^2\kappa^\dagger\kappa\,, \quad (2.10\text{d})$$

and for the spin-one mesons,

$$\mathfrak{L}_{(0)\rho}=-\tfrac{1}{2}(\partial_\mu\rho_{\nu a}-\partial_\nu\rho_{\mu a})\rho^{\mu\nu}{}_a +\tfrac{1}{4}\rho^{\mu\nu}{}_a\rho_{\mu\nu a}-\tfrac{1}{2}m_\rho{}^2\rho_{\mu a}\rho^\mu{}_a\,, \quad (2.10\text{e})$$

[9] The decay constants F_K, etc., are defined by $\langle 0|C_\alpha{}^\mu(0)|K_\beta(k)\rangle =iF_K\delta_{\alpha\beta}Nk^\mu$, where $N\equiv[2\omega_k(2\pi)^3]^{-1/2}$, etc. Similarly, constants g_ρ, etc., are defined by the vacuum one-meson matrix element $\langle 0|V_a{}^\mu(0)|\varphi_b(k)\rangle=g_\rho\delta_{ab}N\epsilon^\mu(k)$, etc. Our metric has signature $+2$, and we use $F_\pi=94$ MeV throughout.

$$\mathcal{L}_{(0)A}=-\tfrac{1}{2}(\partial_\mu a_{\nu a}-\partial_\nu a_{\mu a})a^{\mu\nu}{}_a+\tfrac{1}{4}a^{\mu\nu}{}_a a_{\mu\nu a}-\tfrac{1}{2}m_A{}^2 a_{\mu a}a^\mu{}_a\,, \quad (2.10\text{f})$$

$$\mathcal{L}_{(0)K^*}=-\tfrac{1}{2}[(\partial_\mu K^*{}_\nu-\partial_\nu K^*{}_\mu)^\dagger K^{*\mu\nu}+\text{H.c.}]+\tfrac{1}{2}K^*{}_{\mu\nu}{}^\dagger K^{*\mu\nu}-m_{K^*}{}^2K^*{}_\mu{}^\dagger K^{*\mu}\,, \quad (2.10\text{g})$$

$$\mathcal{L}_{(0)K_A}=-\tfrac{1}{2}[(\partial_\mu K_{A\nu}-\partial_\nu K_{A\mu})^\dagger K_A{}^{\mu\nu}+\text{H.c.}]+\tfrac{1}{2}K_{A\mu\nu}{}^\dagger K_A{}^{\mu\nu}-m_{K_A}{}^2K_{A\mu}{}^\dagger K_A{}^\mu\,. \quad (2.10\text{h})$$

The cubic part of the Lagrangian that enters in the $K\pi$ scattering process is

$$\mathcal{L}_{(3)}=\mathcal{L}_{(3)\text{NS}}+\mathcal{L}_{(3)\text{S}}\,, \quad (2.11)$$

where $\mathcal{L}_{(3)\text{S}}$ contains strange particles and $\mathcal{L}_{(3)\text{NS}}$ contains only nonstrange particles:

$$\begin{aligned}\mathcal{L}_{(3)\text{NS}}=\epsilon_{abc}(&g_{\pi\pi\rho}\pi_b{}^\mu\pi_c\rho_{\mu a}+\tfrac{1}{2}\lambda_{\pi\pi\rho}\pi_{\nu a}\pi_{\mu b}\rho^{\mu\nu}{}_c\\&+\tfrac{1}{2}\lambda_{\rho AA}a_{\mu a}a_{\nu b}\rho^{\nu\mu}{}_c)+\tfrac{1}{2}g_{\sigma\pi\pi}\pi^2\sigma\\&+\tfrac{1}{2}\lambda_{\sigma\pi\pi}\pi^\mu{}_a\pi_{\mu a}\sigma+\mu_{\sigma\pi\pi}\pi_a\pi^\nu{}_a\sigma_\nu\\&+\lambda_{\sigma\pi A}\pi_a a^\mu{}_a\sigma_\mu+\tilde{\lambda}_{\sigma\pi A}\pi^\mu{}_a a_{\mu a}\sigma\,, \quad (2.12\text{a})\end{aligned}$$

$$\begin{aligned}\mathcal{L}_{(3)\text{S}}=i(&g_{KK\rho}K_\mu{}^\dagger\tau K\rho^\mu+\tfrac{1}{2}\lambda_{KK\rho}K_\mu{}^\dagger\tau K_\nu\rho^{\nu\mu}\\&+\tfrac{1}{2}\lambda_{\rho K_AK_A}K_{A\mu}{}^\dagger\tau K_{A\nu}\rho^{\nu\mu}+g_{\pi K\kappa}\kappa^\dagger\tau K\pi+\lambda_{\pi K\kappa}\kappa_\mu{}^\dagger\tau K^\mu\pi\\&+\mu_{\pi K\kappa}\kappa^\dagger\tau K^\mu\pi_\mu+\tilde{\mu}_{\pi K\kappa}\kappa_\mu{}^\dagger\tau K\pi^\mu+\lambda_{\pi KK^*}K^*{}_\mu{}^\dagger\tau K^\mu\pi\\&+g_{\pi KK^*}K^*{}_\mu{}^\dagger\tau K\pi^\mu+\mu_{\pi KK^*}K^*{}_{\nu\mu}{}^\dagger\tau K^\mu\pi^\nu+\lambda_{AK\kappa}\kappa_\mu{}^\dagger\tau Ka^\mu\\&+g_{\pi\kappa K_A}\kappa^\dagger\tau K_A{}^\mu\pi_\mu+\lambda_{\pi\kappa K_A}\kappa_\mu{}^\dagger\tau K_A{}^\mu\pi)+g_{\sigma KK}K^\dagger K\sigma\\&+\lambda_{\sigma KK}K_\mu{}^\dagger K^\mu\sigma+\mu_{\sigma KK}K_\mu{}^\dagger K\sigma^\mu+\lambda_{\sigma KK_A}K_A{}^{\mu\dagger}K\sigma_\mu\\&+\tilde{\lambda}_{\sigma KK_A}K_A{}^{\mu\dagger}K_\mu\sigma+\text{H.c.} \quad (2.12\text{b})\end{aligned}$$

Here $\mathcal{L}_{(3)}$ contains only those terms that contribute directly to the $K\pi$ amplitude.

Since the Lagrangians of Eqs. (2.10) and (2.12) are written in the first-order formalism, (K^μ,K), $(a^{\mu\nu},a^\mu)$, etc., are to be varied independently. The auxiliary fields are determined by Lagrange's equations, which for the scalar fields are

$$\pi^\mu=\partial^\mu\pi-\frac{\delta\mathcal{L}_I}{\delta\pi_\mu}\,, \quad (2.13)$$

$$K^\mu=\partial^\mu K-\frac{\delta\mathcal{L}_I}{\delta K_\mu{}^\dagger}\,, \quad (2.14)$$

etc. Similarly, for the vector fields we have

$$\rho^{\mu\nu}=\partial^\mu\rho^\nu-\partial^\nu\rho^\mu-2\frac{\delta\mathcal{L}_I}{\delta\rho_{\mu\nu}}\,, \quad (2.15)$$

$$K^{*\mu\nu}=\partial^\mu K^{*\nu}-\partial^\nu K^{*\mu}-2\frac{\delta\mathcal{L}_I}{\delta K^*{}_{\mu\nu}{}^\dagger}\,, \quad (2.16)$$

etc.

The field-current identities (2.6) and the equations of motion are used to compute the divergences and commutators of V, A, C, and S. These currents are functions of the couplings in $\mathcal{L}_{(3)}$. Thus, constraints on the coupling constants are obtained by requiring the chiral current algebra (2.1) and the PCC to hold. The satisfaction of these conditions requires that the constants of $\mathcal{L}_{(3)\text{NS}}$ obey the relations[2,4]

$$g_{\pi\pi\rho}=m_\rho{}^2/g_\rho\,, \quad (2.17\text{a})$$

$$g_\rho\lambda_{\pi\pi\rho}=1-g_A{}^2(F_\pi{}^2m_A{}^2)^{-1}+g_A{}^2m_\rho{}^2(F_\pi{}^2m_A{}^4)^{-1}\lambda_A\,, \quad (2.17\text{b})$$

$$F_\pi g_{\sigma\pi\pi}=m_\sigma{}^2\lambda_3-m_\pi{}^2\lambda_1\,, \quad (2.17\text{c})$$

$$F_\pi\lambda_{\sigma\pi\pi}=-(\lambda_1+\lambda_2)\,, \quad (2.17\text{d})$$

$$g_\rho{}^2m_\rho{}^{-2}-g_A{}^2m_A{}^{-2}=F_\pi{}^2\,, \quad (2.17\text{e})$$

where $\lambda_A\equiv g_\rho m_\rho{}^{-2}\lambda_{\rho AA}$ is the anomalous moment of the A_1 meson and

$$\lambda_1\equiv(g_Am_A{}^{-2})\lambda_{\sigma\pi A}\,,\quad \lambda_2\equiv(g_Am_A{}^{-2})\tilde{\lambda}_{\sigma\pi A}\,,\quad \lambda_3\equiv\lambda_1+F_\pi\mu_{\sigma\pi\pi}\,. \quad (2.18)$$

Similarly, for $\mathcal{L}_{(3)\text{S}}$ we have

$$g_{KK\rho}=\tfrac{1}{2}m_\rho{}^2/g_\rho\,,$$
$$g_\rho\lambda_{KK\rho}=1-g_{K_A}{}^2(F_K{}^2m_{K_A}{}^2)^{-1}+g_{K_A}{}^2m_\rho{}^2(F_K{}^2m_{K_A}{}^4)^{-1}\lambda_{K_A}\,, \quad (2.19)$$

where $\lambda_{K_A}\equiv g_\rho m_\rho{}^{-2}\lambda_{\rho K_AK_A}$. For the K-σ couplings,

$$F_Kg_{\sigma KK}=m_\sigma{}^2\gamma_3-m_K{}^2\gamma_1\,,\quad F_K\lambda_{\sigma KK}=-(\gamma_1+\gamma_2)\,, \quad (2.20\text{a})$$

where

$$\gamma_1\equiv g_{K_A}m_{K_A}{}^{-2}\lambda_{\sigma KK_A}\,,\quad \gamma_2\equiv g_{K_A}m_{K_A}{}^{-2}\tilde{\lambda}_{\sigma KK_A}\,,\quad \gamma_3\equiv\gamma_1+F_K\mu_{\sigma KK}\,. \quad (2.20\text{b})$$

For the π-K-κ couplings

$$\lambda_{\pi K\kappa}=f[\alpha(1+m_\kappa{}^2/m_K{}^2)F_K{}^2-F_K{}^2+F_\kappa{}^2+L_{\pi\kappa K}+L_{K\pi\kappa}]\,, \quad (2.21\text{a})$$

$$\mu_{\pi K\kappa}=f[\alpha(m_\kappa{}^2/m_\pi{}^2+m_\kappa{}^2/m_K{}^2)F_K{}^2+F_K{}^2-F_\pi{}^2+L_{\kappa K\pi}+L_{\pi\kappa K}]\,, \quad (2.21\text{b})$$

$$\tilde{\mu}_{\pi K\kappa}=f[\alpha(m_\kappa{}^2/m_\pi{}^2+1)F_K{}^2+F_\pi{}^2-F_\kappa{}^2+L_{K\pi\kappa}+L_{\kappa K\pi}]\,, \quad (2.21\text{c})$$

where

$$L_{abc}\equiv(m_a{}^2F_a{}^2-m_b{}^2F_b{}^2)m_c{}^{-2}\,,\quad \alpha\equiv2F_\kappa F_\pi(F_Km_\kappa{}^2)^{-1}g_{\pi K\kappa}\,,\quad f^{-1}\equiv4F_\pi F_KF_\kappa\,. \quad (2.21\text{d})$$

Here α governs the width of the κ meson and in part determines the breakdown of the ordinary $SU(3)$ symmetry. For the π-K-K^* couplings

$$g_{\pi KK^*}=\left(\frac{m_{K^*}{}^2}{g_{K^*}}F_\kappa\right)\times f(-\alpha F_K{}^2+F_\kappa{}^2-2F_\pi{}^2+L_{\pi K\kappa})\,, \quad (2.22\text{a})$$

$$\lambda_{\pi KK^*}=\left(\frac{m_{K^*}{}^2}{g_{K^*}}F_\kappa\right)\times f(-\alpha F_K{}^2+2F_K{}^2-F_\kappa{}^2+L_{\pi K\kappa})\,, \quad (2.22\text{b})$$

where $\lambda_s\equiv4F_\pi g_{K^*}\mu_{\pi KK^*}/F_K$ is the strange-meson analog of λ_A, and

$$\lambda_{AK\kappa}=\left(\frac{m_A{}^2}{g_A}F_\pi\right)f(-\alpha F_K{}^2m_\kappa{}^2/m_\pi{}^2+2F_\kappa{}^2-F_\pi{}^2+L_{K\kappa\pi}),\quad(2.23\text{a})$$

$$g_{\pi\kappa K_A}=\left(\frac{m_{K_A}{}^2}{g_{K_A}}F_K\right)f(-\alpha F_K{}^2m_\kappa{}^2/m_K{}^2+2F_\pi{}^2-F_K{}^2+L_{\kappa\pi K}),\quad(2.23\text{b})$$

$$\lambda_{\pi\kappa K_A}=\left(\frac{m_{K_A}{}^2}{g_{K_A}}F_K\right)f(-\alpha F_K{}^2m_\kappa{}^2/m_K{}^2+F_K{}^2-2F_\kappa{}^2+L_{\kappa\pi K}).\quad(2.23\text{c})$$

Finally, the first Weinberg[10] sum rule

$$g_\rho{}^2m_\rho{}^{-2}=F_\pi{}^2+g_A{}^2m_A{}^{-2}=F_K{}^2+g_{K_A}{}^2m_{K_A}{}^{-2}=F_\kappa{}^2+g_{K^*}{}^2m_{K^*}{}^{-2}\quad(2.24)$$

arises as a consequence of the assumption that the q-number Schwinger terms in Eq. (2.1) all vanish. The three-point coupling constants are determined by the current algebra conditions in terms of λ_A, λ_1, λ_2, λ_3, λ_s, γ_1, γ_2, γ_3, λ_{K_A}, and α. Of these, λ_A and λ_s may be obtained from a knowledge of the ρ-meson and K^*-meson widths, respectively. Further, the combinations $\lambda_1-\lambda_2+2(m_\pi{}^2/m_\sigma{}^2)\lambda_2$ and $\gamma_1-\gamma_2+2(m_K{}^2/m_\sigma{}^2)\gamma_2$ enter into the σ width, while α governs the width of the κ. At present there is no way of experimentally determining λ_{K_A}; hence it shall be set to zero for the remainder of this work.

In extending the above considerations to the four-point functions, we make a dynamical assumption in addition to that of single particle saturation of T-products. This assumption concerns the σ commutators

$$\delta(x^0-y^0)[\pi_a(x),A^0{}_b(y)]=\delta^4(x-y)\sigma_{ab}{}^\pi(x),\text{ etc.}\quad(2.25)$$

Since single-meson saturation has been assumed for other aspects of the analysis, a natural extension seems to be to postulate that the σ commutators of Eq. (2.25) are single-meson dominated; i.e., governed by a resonance pole. The σ meson itself appears to be the only resonance with the correct quantum numbers available for this purpose. Thus we assume that

$$\delta(x^0-y^0)[\pi_a(x),A^0{}_b(y)]\sim\delta^4(x-y)\delta_{ab}\sigma(x),\text{ etc.}\quad(2.26)$$

The dynamical assumption of Eq. (2.26) is most easily achieved if V^0, A^0, C^0, and S^0 are restricted to be at most quadratic functions of the canonical variables. The satisfaction of Eqs. (2.1) to order g^2 then produces the following additional restrictions on the coupling constants of $\mathcal{L}_{(3)}$[4,7,11]:

$$\lambda_1\lambda_3=1,\quad(2.27\text{a})$$

$$\lambda_1\gamma_3=F_\kappa f[-\alpha(m_\kappa{}^2/m_\pi{}^2)F_K{}^2+F_\pi{}^2+L_{K\kappa\pi}],\quad(2.27\text{b})$$

$$\lambda_3\gamma_1=F_\kappa f[-\alpha(m_\kappa{}^2/m_K{}^2)F_K{}^2+F_K{}^2+L_{\pi\kappa K}],\quad(2.27\text{c})$$

$$\alpha^2=\frac{m_K{}^4}{m_\kappa{}^4}\left(1-\frac{m_\pi{}^2}{m_K{}^2}\frac{F_\pi{}^2}{F_K{}^2}\right)^2+\frac{F_\kappa{}^2}{F_K{}^2}\left(\frac{F_\kappa{}^2}{F_K{}^2}-2\frac{m_K{}^2}{m_\kappa{}^2}-2\frac{m_\pi{}^2}{m_\kappa{}^2}\frac{F_\pi{}^2}{F_K{}^2}\right).\quad(2.27\text{d})$$

Equations (2.27a)–(2.27c) determine some of the σ couplings in terms of the κ width parameter α. Equation (2.27d) produces restrictions on the mass of the κ meson, in particular[7,11–13]

$$|F_\kappa m_\kappa|>|F_Km_K|+|F_\pi m_\pi|\quad\text{and}\quad|F_\kappa m_\kappa|<|F_Km_K|-|F_\pi m_\pi|.\quad(2.28)$$

These restrictions may be combined with information on the K_{l3} form factor $f_+(0)$ to relate the width and mass of the κ meson to the ratio F_K/F_π. The hard-meson analysis of K_{l3} decay[5,6] determines $f_+(0)$ to be

$$f_+(0)=2(F_\pi F_K)^{-1}(F_\pi{}^2+F_K{}^2-F_\kappa{}^2).\quad(2.29)$$

The experimental information of Trippe *et al.*[14] indicates a κ meson with $m_\kappa\simeq1100$–1200 MeV. Using the experimental value $F_K/[F_\pi f_+(0)]=1.23\pm0.03$,[15] and setting $m_\kappa=1100$ MeV and $\Gamma(\kappa\to K\pi)=450$ MeV, one obtains $F_\kappa/F_\pi=0.380$ and $F_K/F_\pi=1.169$. The narrow κ width of 90 ± 30 MeV (and $m_\kappa=1150$ MeV) given by Crennell *et al.*[16] is not compatible with Eqs. (2.27d) and (2.29), since the current algebra, with a pole-dominated σ commutator, demands that a κ meson of 1100 MeV have a width greater than 450 MeV. As the value of $F_K/F_\pi f_+(0)$ increases (decreases) the κ width and the maximum allowed value of F_K/F_π increases (decreases). For the experimental value of $F_K/F_\pi f_+(0)$ quoted here, the value of F_K/F_π that ensures the reality of F_κ demands $F_K/F_\pi\leq1.260$ and the reality of α demands $F_K/F_\pi\geq1.161$. Using $F_\kappa/F_\pi=0.38$ and $F_K/F_\pi=1.169$, we find from Eqs. (2.27) that $\lambda_1\gamma_3=1.120$, $\lambda_3\gamma_1=0.223$, and $\alpha=0.0464$ in order that the current algebra be exactly satisfied by quadratic currents.

Using the pole dominance of the σ commutators, an $\mathcal{L}_{(4)}$ consistent with the current-algebra restrictions can be easily constructed.[7,11] The relevant part of $\mathcal{L}_{(4)}$ that enters in the $K\pi$ scattering is given as

$$\mathcal{L}_{(4)}=G_1K^\dagger K\pi^2+G_2K_\mu{}^\dagger K^\mu\pi^2+G_3K^\dagger K\pi^\mu{}_a\pi_{\mu a}+G_4(K_\mu{}^\dagger K+K^\dagger K_\mu)\pi^\mu{}_a\pi_a+iG_5\epsilon_{abc}(K^\dagger\tau_cK_\mu-K_\mu{}^\dagger\tau_cK)\pi^\mu{}_b\pi_a,\quad(2.30)$$

[10] S. Weinberg, Phys. Rev. Letters **18**, 507 (1967).

[11] L. K. Pande, Phys. Rev. **184**, 1683 (1969).

[12] This result was first obtained under the assumption that symmetry breakdown corresponds to a $(3,3^*)+(3^*,3)$ term in the interaction (see Ref. 13). It can be shown generally that the pole dominance of the σ-commutators when coupled with the current-algebra constraints lead to a $(3,3^*)+(3^*,3)$ breakdown (Ref. 13). A similar conclusion was obtained by L. K. Pande, Phys. Rev. Letters **23**, 353 (1969).

[13] S. Glashow and S. Weinberg, Phys. Rev. Letters **20**, 224 (1968).

[14] T. G. Trippe, C.-Y. Chien, E. Mellema, P. E. Schlein, W. E. Slater, D. H. Stork, and H. K. Ticho, Phys. Rev. Letters **28B**, 203 (1968).

[15] N. Breene (unpublished).

[16] D. J. Crennell, Uri Karshon, K. W. Lai, J. S. O'Neall, and J. M. Scarr, Phys. Rev. Letters **22**, 487 (1969).

where the G's are of second order in the $\mathfrak{L}_{(3)}$ constants:

$$G_1=g_{\pi K\kappa}\left(\frac{g_A}{m_A{}^2F_\pi}\lambda_{AK\kappa}+\tilde{\mu}_{\pi K\kappa}\right)-\frac{\lambda_3}{2F_\pi}g_{\sigma KK}\,, \tag{2.31a}$$

$$G_2=\lambda_{\pi K\kappa}\left(\frac{g_A}{m_A{}^2F_\pi}g_{AK\kappa}+\mu_{\pi K\kappa}\right)-\frac{(\lambda_{\pi KK^*})^2}{m_{K^*}{}^2}-\frac{\lambda_3}{2F_\pi}\lambda_{\sigma KK}\,, \tag{2.31b}$$

$$G_3=\tilde{\mu}_{\pi K\kappa}\left(\frac{g_{KA}}{m_{KA}{}^2F_K}g_{\pi\kappa K_A}+\mu_{\pi K\kappa}\right)-\frac{(g_{\pi KK^*})^2}{m_{K^*}{}^2}-\frac{\gamma_3}{2F_K}\lambda_{\sigma\pi\pi}\,, \tag{2.31c}$$

$$G_4=-\mu_{\pi K\kappa}\left(\frac{g_A}{m_A{}^2F_\pi}\lambda_{AK\kappa}+\tilde{\mu}_{\pi K\kappa}\right)+\tilde{\mu}_{\pi K\kappa}\left(\frac{g_A}{m_A{}^2F_\pi}g_{AK\kappa}+\mu_{\pi K\kappa}\right)-\frac{\lambda_{\pi KK^*}g_{\pi KK^*}}{m_{K^*}{}^2}-\frac{\lambda_1}{F_\pi}\mu_{\sigma KK}\,, \tag{2.31d}$$

$$G_5=-\mu_{\pi K\kappa}\left(\frac{g_A}{m_A{}^2F_\pi}\lambda_{AK\kappa}+\tilde{\mu}_{\pi K\kappa}\right)-\tilde{\mu}_{\pi K\kappa}\left(\frac{g_A}{m_A{}^2F_\pi}g_{AK\kappa}+\mu_{\pi K\kappa}\right)+\frac{\lambda_{\pi KK^*}g_{\pi KK^*}}{m_{K^*}{}^2}-\frac{g_{\pi\pi\rho}g_{KK\rho}}{m_\rho{}^2}\,. \tag{2.31e}$$

All the coupling constants appearing in Eqs. (2.31) have already been defined in our discussion of $\mathfrak{L}_{(3)}$.

III. $K\pi$ SCATTERING AMPLITUDES

In this section we shall use the formalism of Sec. II to calculate the $K\pi$ scattering amplitudes. Of particular interest are the S- and P-wave partial amplitudes, which we calculate explicitly, as well as the S- and P-wave scattering lengths and S-wave effective ranges. As discussed in Secs. I and II, the hard-meson technique requires that we use the effective Lagrangian only to second order in calculating the scattering amplitude. A convenient way of calculating the S-matrix element $\langle K_\beta(p_1)\pi_b(p_2)\text{ out}|K_\alpha(q_1)\pi_a(q_2)\text{ in}\rangle$ is to contract the incoming pion $\pi_a(q_2)$ to obtain

$$\langle K_\beta(p_1)\pi_b(p_2)|K_\alpha(q_1)\pi_a(q_2)\rangle=-i[2\omega_{q_2}(2\pi)^3]^{-1/2}\times\int d^4y\; e^{iq_2y}\langle K_\beta(p_1)\pi_b(p_2)|\mathcal{J}_a(y)|K_\alpha(q_1)\rangle\,, \tag{3.1}$$

where $\mathcal{J}_a(y)$ is the pion field equation source term, i.e.,

$$(-\Box^2+m_\pi{}^2)\pi_a(y)=\mathcal{J}_a(y)\,. \tag{3.2}$$

This source term may be written as the sum of a pole part and a seagull part:

$$\mathcal{J}_a(y)=\mathcal{J}_a{}^{\mathrm{P}}(y)+\mathcal{J}_a{}^{\mathrm{SG}}(y)\,. \tag{3.3a}$$

$\mathfrak{L}_{(4)}$ produces contributions to $\mathcal{J}_a$ which are cubic in the field variables and hence contributes only to the seagull portion of Eq. (3.3a). $\mathfrak{L}_{(3)}$ in the first-order formalism contributes to both the pole and the seagull parts of $\mathcal{J}_a$. In general, $\mathfrak{L}_{(3)}$ produces in $\mathcal{J}_a$ quadratic functions in the fields π, π_μ; K, K_μ; etc. When the auxiliary fields π_μ, K_μ, etc., are eliminated by the first-order equations (2.13)–(2.16), cubic structures in the field variables (second order in the coupling constants) will result. Thus by Eqs. (2.9) and (2.12), the pole part is

$$\begin{aligned}\mathcal{J}_a{}^{\mathrm{P}}(y)=&(2g_{\pi\pi\rho}-m_\rho{}^2\lambda_{\pi\pi\rho})\epsilon_{abc}\partial^\mu\pi_c\rho_{\mu b}+(g_{\sigma\pi\pi}-m_\sigma{}^2\mu_{\sigma\pi\pi}-m_\pi{}^2\lambda_{\sigma\pi\pi})\pi_a\sigma\\&-\lambda_{\sigma\pi\pi}\partial^\mu\pi_a\partial_\mu\sigma+i(-g_{\pi K\kappa}+m_K{}^2\mu_{\pi K\kappa}+m_\kappa{}^2\tilde{\mu}_{\pi K\kappa})(K^\dagger\tau_a\kappa-\kappa^\dagger\tau_aK)+i(-\lambda_{\pi K\kappa}+\mu_{\pi K\kappa}+\tilde{\mu}_{\pi K\kappa})\\&\times(\partial^\mu K^\dagger\tau_a\partial_\mu\kappa-\partial_\mu\kappa^\dagger\tau_a\partial^\mu K)+i(-\lambda_{\pi KK^*}+g_{\pi KK^*}+m_{K^*}{}^2\mu_{\pi KK^*})(\partial^\mu K^\dagger\tau_aK^*{}_\mu-K^*{}_\mu{}^\dagger\tau_a\partial^\mu K)\,.\end{aligned} \tag{3.3b}$$

The seagull part to second order in the coupling constants is

$$\begin{aligned}\mathcal{J}_a{}^{\mathrm{SG}}(y)=&\Bigg[-\frac{\lambda_1}{F_\pi}(g_{\sigma KK}-2m_K{}^2\mu_{\sigma\pi\pi})+\frac{\gamma_3}{F_K}m_\pi{}^2\lambda_{\sigma\pi\pi}-2m_\pi{}^2\tilde{\mu}_{\pi K\kappa}\left(\tilde{\mu}_{\pi K\kappa}+\frac{g_{K_A}}{F_Km_{K_A}{}^2}g_{\pi\kappa K_A}\right)\\&+2(-g_{\pi K\kappa}+m_K{}^2\mu_{\pi K\kappa}+m_\kappa{}^2\tilde{\mu}_{\pi K\kappa})\left(\tilde{\mu}_{\pi K\kappa}+\frac{g_A}{F_\pi m_A{}^2}\lambda_{AK\kappa}\right)\Bigg]K^+K\pi_a+\Bigg[-\frac{\lambda_1}{F_\pi}(\lambda_{\sigma KK}-2\mu_{\sigma KK})\\&+2(-\lambda_{\pi K\kappa}+\tilde{\mu}_{\pi K\kappa}+\mu_{\pi K\kappa})\left(\tilde{\mu}_{\pi K\kappa}+\frac{g_A}{F_\pi m_A{}^2}\lambda_{AK\kappa}\right)-2\frac{\lambda_{\pi KK^*}}{m_{K^*}{}^2}(\lambda_{\pi KK^*}-g_{\pi KK^*}-m_{K^*}{}^2\mu_{\pi KK^*})\Bigg]\partial^\mu K^\dagger\partial_\mu K\pi_a\\&+\Bigg[\frac{\gamma_3}{F_K}\lambda_{\sigma\pi\pi}-\tilde{\mu}_{\pi K\kappa}\left(\lambda_{\pi K\kappa}+\mu_{\pi K\kappa}-\tilde{\mu}_{\pi K\kappa}+2\frac{g_{K_A}}{F_Km_{K_A}{}^2}g_{\pi\kappa K_A}\right)-\frac{g_{\pi KK^*}}{m_{K^*}{}^2}(\lambda_{\pi KK^*}-g_{\pi KK^*}-m_{K^*}{}^2\mu_{\pi KK^*})\Bigg]\\&\times(\partial^\mu K^\dagger K+K^\dagger\partial^\mu K)\partial_\mu\pi_a+\Bigg[-\frac{1}{2g_\rho}(2g_{\pi\pi\rho}-m_\rho{}^2\lambda_{\pi\pi\rho})+2(-\mu_{\pi K\kappa}+\lambda_{\pi K\kappa})\left(\lambda_{\pi K\kappa}+\frac{g_{K_A}}{F_Km_{K_A}{}^2}\lambda_{\pi\kappa K_A}\right)\\&-\tilde{\mu}_{\pi K\kappa}(-\mu_{\pi K\kappa}+\lambda_{\pi K\kappa}+\tilde{\mu}_{\pi K\kappa})+\frac{g_{\pi KK^*}}{m_{K^*}{}^2}(\lambda_{\pi KK^*}-g_{\pi KK^*}-m_{K^*}{}^2\mu_{\pi KK^*})\Bigg]i\epsilon_{abc}(K^\dagger\tau_c\partial^\mu K-\partial^\mu K^\dagger\tau_cK)\partial_\mu\pi_b\,.\end{aligned} \tag{3.3c}$$

Only those terms in Eq. (3.3c) which contribute to $K\pi$ scattering are retained. The definitions of the σ-couplings λ_1, γ_3 given by Eqs. (2.18) and (2.20) have been used.

The contribution of the seagull portion of the source term is obtained straightforwardly by approximating the kaon and pion fields by free fields. The pole part is only a linear function of the coupling constants. Consequently, the fields must be expanded to one more order to produce a second-order contribution to the S matrix. The field equations are computed from Eqs. (2.9)–(2.12) and we find

$$\begin{aligned}&[(-\Box^2+m_\rho{}^2)\delta^\mu{}_\nu+\partial^\mu\partial_\nu]\rho^\nu{}_a(x)\\&\quad=+ig_{KK\rho}(\partial^\mu K^\dagger\tau_a K-K^\dagger\tau_a\partial^\mu K)\\&\qquad+i\lambda_{KK\rho}\partial_\lambda(\partial^\lambda K^\dagger\tau_a\partial^\mu K-\partial^\mu K^\dagger\tau_a\partial^\lambda K)\,,\end{aligned}\tag{3.4}$$

$$\begin{aligned}(-\Box^2+m_\sigma{}^2)\sigma(x)&=(g_{\sigma KK}-2m_K{}^2\mu_{\sigma KK})K^\dagger K\\&\quad+(\lambda_{\sigma KK}-2\mu_{\sigma KK})\partial^\mu K^\dagger\partial_\mu K\,,\end{aligned}\tag{3.5}$$

$$\begin{aligned}&[(-\Box^2+m_{K^*}{}^2)\delta^\mu{}_\nu+\partial^\mu\partial_\nu]K^{*\nu}\\&\quad=i\lambda_{\pi KK^*}\tau\partial^\mu K\pi+ig_{\pi KK^*}\tau K\partial^\mu\pi\\&\qquad-i\mu_{\pi KK^*}\tau\partial_\nu(\partial^\mu K\partial^\nu\pi-\partial^\nu K\partial^\mu\pi)\,,\end{aligned}\tag{3.6}$$

$$\begin{aligned}(-\Box+m_\kappa{}^2)\kappa(x)&=+i(g_{\pi K\kappa}-m_K{}^2\lambda_{\pi K\kappa}-m_\pi{}^2\tilde{\mu}_{\pi K\kappa})\\&\quad\times\tau K\pi+i(\mu_{\pi K\kappa}-\lambda_{\pi K\kappa}-\tilde{\mu}_{\pi K\kappa})\tau\partial^\mu K\partial_\mu\pi\,,\end{aligned}\tag{3.7}$$

where only those terms have been kept on the right-hand side that give the desired contribution to Eq. (3.1). Then by inserting the first-order solutions to Eqs. (3.4)–(3.7) into $\mathcal{J}_a{}^{\mathrm{P}}$, the total $\mathcal{J}_a{}^{\mathrm{P}}$ valid to second order is obtained. The above structures give rise to direct- and crossed-channel κ and K^* poles and crossed-channel σ and ρ poles.

A. Total Amplitudes

The scattering matrix is computed by defining the function $M_{\beta,b;\alpha,a}$ as

$$\begin{aligned}\langle K_\beta(p_1)\pi_b(p_2)|K_\alpha(q_1)\pi_a(q_2)\rangle&=i(2\pi)^4\delta^4(p_1+p_2-q_1-q_2)\\&\quad\times[16\omega_{q_1}\omega_{q_2}\omega_{p_1}\omega_{p_2}(2\pi)^{12}]^{-1/2}M_{\beta,b;\alpha,a}\,.\end{aligned}\tag{3.8}$$

As a consequence of isospin and crossing symmetry, M has the form

$$\begin{aligned}M_{\beta,b;\beta,a}&=\delta_{\beta\alpha}\delta_{ba}A^{(+)}(s,t,u)\\&\quad+i\epsilon_{bac}(\tau_c)_{\beta\alpha}A^{(-)}(s,t,u)\,,\end{aligned}\tag{3.9a}$$

where

$$A^{(\pm)}(s,t,u)=\pm A^{(\pm)}(u,t,s)\,,\tag{3.9b}$$

and the invariants s, t, and u are defined by

$$\begin{aligned}s&\equiv-(q_1+q_2)^2=-(p_1+p_2)^2\,,\\t&\equiv-(q_1-p_1)^2=-(q_2-p_2)^2\,,\\u&\equiv-(q_1-p_2)^2=-(p_1-q_2)^2\,.\end{aligned}\tag{3.10}$$

By a straightforward calculation the even amplitude $A^{(+)}$ is found to have the form

$$\begin{aligned}A^{(+)}(s,t,u)&=Z_1+Z_2t+Z_3(s+u)\\&\quad+Z_4\frac{1}{-t+m_\sigma{}^2}+Z_5\left(\frac{1}{-s+m_\kappa{}^2}+\frac{1}{-u+m_\kappa{}^2}\right)\\&\quad+\left[(Z_6+Z_7u+Z_8t)\frac{1}{-s+m_{K^*}{}^2}+s\leftrightarrow u\right],\end{aligned}\tag{3.11a}$$

and the odd amplitude $A^{(-)}$ is determined to be

$$\begin{aligned}A^{(-)}(s,t,u)&=Z_{10}(u-s)\\&\quad+Z_{11}\frac{u-s}{-t+m_\rho{}^2}+Z_5\left(\frac{1}{-s+m_\kappa{}^2}-\frac{1}{-u+m_\kappa{}^2}\right)\\&\quad+\left[(Z_6+Z_7u+Z_8t)\frac{1}{-s+m_{K^*}{}^2}-s\leftrightarrow u\right].\end{aligned}\tag{3.11b}$$

We now discuss the constants Z_1–Z_{11}. We first consider the constants appearing with the various poles in Eqs. (3.11). For the σ pole,

$$\begin{aligned}Z_4&=\frac{m_\sigma{}^4}{4F_\pi F_K}\left(\lambda_1-\lambda_2+2\frac{m_\pi{}^2}{m_\sigma{}^2}\lambda_2\right)\\&\quad\times\left(\gamma_1-\gamma_2+2\frac{m_K{}^2}{m_\sigma{}^2}\gamma_2\right);\end{aligned}\tag{3.12}$$

for the κ pole,

$$Z_5=\frac{m_\kappa{}^4}{4F_\kappa{}^2}G^2\,,\tag{3.13}$$

$$\begin{aligned}G&\equiv(2F_\pi F_K)^{-1}\bigg[F_K{}^2(1-\alpha)+\frac{m_K{}^2}{m_\kappa{}^2}F_\pi{}^2-F_\pi{}^2\\&\quad-m_\kappa{}^{-2}(m_K{}^2-m_\pi{}^2)F_\kappa{}^2-\frac{m_\pi{}^2}{m_\kappa{}^2}F_K{}^2\bigg];\end{aligned}$$

for the K^* pole,

$$\begin{aligned}Z_7&=-\tfrac{1}{4}(-g_{\pi KK^*}+\lambda_{\pi KK^*}-m_{K^*}{}^2\mu_{\pi KK^*})^2\\&\quad\times\left(1+\frac{m_K{}^2}{m_{K^*}{}^2}-\frac{m_\pi{}^2}{m_{K^*}{}^2}\right),\end{aligned}\tag{3.14a}$$

$$\begin{aligned}Z_8&=\tfrac{1}{4}(-g_{\pi KK^*}+\lambda_{\pi KK^*}-m_{K^*}{}^2\mu_{\pi KK^*})^2\\&\quad\times\left(1-\frac{m_K{}^2}{m_{K^*}{}^2}+\frac{m_\pi{}^2}{m_{K^*}{}^2}\right),\end{aligned}\tag{3.14b}$$

$$\begin{aligned}Z_6&=-(Z_7+Z_8)(m_K{}^2+m_\pi{}^2-\tfrac{1}{2}m_{K^*}{}^2)\\&\quad+(Z_8-Z_7)\frac{(m_K{}^2-m_\pi{}^2)^2}{2m_{K^*}{}^2},\end{aligned}\tag{3.14c}$$

$$-g_{\pi KK^*}+\lambda_{\pi KK^*}-m_{K^*}{}^2\mu_{\pi KK^*}=\frac{m_{K^*}{}^2}{g_{K^*}}\left(f_+(0)-\frac{F_K}{4F_\pi}\lambda_s\right), \quad (3.14d)$$

where $f_+(0)$ is defined in Eq. (2.29). For the ρ pole,

$$Z_{11}=-(g_{\pi\pi\rho}-\tfrac{1}{2}m_\rho{}^2\lambda_{\pi\pi\rho})(g_{KK\rho}-\tfrac{1}{2}m_\rho{}^2\lambda_{KK\rho}). \quad (3.15)$$

Next we discuss the constants connected with the seagull contribution to the amplitudes of Eq. (3.11). For the odd amplitude,

$$Z_{10}=-Z_{11}m_\rho{}^{-2}+\tfrac{1}{2}(Z_8-Z_7)m_{K^*}{}^{-2}+\frac{1}{8F_K{}^2}\left[-1-\frac{F_K{}^2}{F_\pi{}^2}+\frac{1}{2}\frac{F_\kappa{}^2}{F_\pi{}^2}+\frac{1}{4}\frac{F_\pi{}^2}{F_\kappa{}^2}\left(\frac{F_K{}^2}{F_\pi{}^2}-1\right)^2\right]. \quad (3.16)$$

For the even amplitude

$$Z_3=\frac{1}{2m_{K^*}{}^2}(-g_{\pi KK^*}+\lambda_{\pi KK^*}-m_{K^*}{}^2\mu_{\pi KK^*})(g_{\pi KK^*}+\lambda_{\pi KK^*}-m_{K^*}{}^2\mu_{\pi KK^*})+\tfrac{1}{4}(\lambda_{\pi K\kappa}-\mu_{\pi K\kappa}-\tilde{\mu}_{\pi K\kappa})(-\lambda_{\pi K\kappa}+\mu_{\pi K\kappa}-\tilde{\mu}_{\pi K\kappa}), \quad (3.17a)$$

$$Z_2=(Z_7-Z_8)m_{K^*}{}^{-2}+\frac{1}{2m_{K^*}{}^2}g_{\pi KK^*}(-g_{\pi KK^*}+\lambda_{\pi KK^*}-m_{K^*}{}^2\mu_{\pi KK^*})+\frac{1}{F_\pi F_K}\lambda_1\gamma_3-\frac{1}{4F_\pi F_K}(\lambda_1-\lambda_2)(\gamma_1-\gamma_2)$$
$$+(-\lambda_{\pi K\kappa}+\mu_{\pi K\kappa}+\tilde{\mu}_{\pi K\kappa})\left(\frac{g_A}{m_A{}^2F_\pi}\lambda_{AK\kappa}+\tilde{\mu}_{\pi K\kappa}\right)+\tilde{\mu}_{\pi K\kappa}\frac{F_\pi}{4F_KF_\kappa}\left(1-\frac{F_K{}^2}{F_\pi{}^2}+\frac{F_\kappa{}^2}{F_\pi{}^2}\right), \quad (3.17b)$$

$$Z_1=-2(m_\pi{}^2+m_K{}^2)Z_3-Z_4m_\sigma{}^{-2}-2Z_5\frac{1}{m_\kappa{}^2-m_K{}^2}-2(Z_7-Z_8)\frac{m_K{}^2}{m_{K^*}{}^2}-\frac{m_\pi{}^2}{F_\pi F_K}\left(\lambda_1\gamma_3-\frac{m_K{}^2}{m_\sigma{}^2}\lambda_2\gamma_2\right)$$
$$-m_\pi{}^2\tilde{\mu}_{\pi K\kappa}\frac{F_\pi}{2F_KF_\kappa}\left(1-\frac{F_K{}^2}{F_\pi{}^2}+\frac{F_\kappa{}^2}{F_\pi{}^2}\right)+m_\pi{}^2(-\lambda_{\pi K\kappa}+\mu_{\pi K\kappa}+\tilde{\mu}_{\pi K\kappa})\left(+\frac{m_\kappa{}^2}{m_\kappa{}^2-m_K{}^2}\frac{G}{2F_\kappa}-\frac{g_A}{m_A{}^2F_\pi}\lambda_{AK\kappa}-\tilde{\mu}_{\pi K\kappa}\right). \quad (3.17c)$$

In order to see the size of the contribution to the total amplitudes from the individual terms in $A^{(\pm)}$, a numerical evaluation of the Z's is recorded:

$$\begin{aligned}
Z_1&=-35.167\,, & Z_6m_{K^*}{}^{-2}&=-0.130\,,\\
m_\pi{}^2Z_2&=-0.120\,, & Z_7&=-1.148\,,\\
(m_\pi{}^2+m_K{}^2)Z_3&=+1.273\,, & Z_8&=+0.644\,,\\
Z_4m_\sigma{}^{-2}&=+2.159\,, & m_\pi m_KZ_{10}&=+0.401\,,\\
Z_5m_\kappa{}^{-2}&=+9.017\,, & Z_{11}&=-6.716\,,
\end{aligned} \quad (3.18)$$

where all of the products are dimensionless. In this evaluation we have used $F_K/F_\pi=1.169$, $F_\kappa/F_\pi=0.380$, $\Gamma(\kappa\to K\pi)=450$ MeV; $\Gamma(K^*\to K\pi)=50$ MeV, $\lambda_A=\frac{1}{2}$, $\lambda_s=0.088$, $m_\sigma=730$ MeV, $\lambda_1{}^2=\frac{3}{4}$, $\lambda_2=0$, $\gamma_2=0$, $\sqrt{2}m_\rho/m_A=1$, $g_A/g_\rho=1$, $g_\rho/(F_\pi\sqrt{2}m_\rho)=1$, and $F_K/F_\pi f_{+(0)}=1.23$. Throughout the remainder of this paper, only the parameter F_K/F_π [and hence F_κ/F_π and $\Gamma(\kappa\to K\pi)$] will be varied.

B. Partial-Wave Amplitudes

Equation (3.11) can be used to form the s-channel $I=\frac{1}{2}$, $\frac{3}{2}$ isospin amplitudes $M^I(s,t)$. According to the usual relations, we obtain

$$M^{1/2}(s,t)=A^{(+)}(s,t,u)+2A^{(-)}(s,t,u)\,, \quad (3.19a)$$

$$M^{3/2}(s,t)=A^{(+)}(s,t,u)-A^{(-)}(s,t,u)\,. \quad (3.19b)$$

$M^{1/2}$ contains direct κ and K^* poles and crossed κ, K^*, ρ, and σ poles. $M^{3/2}$ contains crossed poles only. The M^I may be expanded in partial waves as

$$M^I(s,t)=8\pi\sum_l(2l+1)A^I{}_l(s)P_l(Z)\,, \quad (3.20a)$$

where

$$A^I{}_l(s)\equiv(s^{1/2}/k)e^{i\delta^I{}_l(s)}\sin\delta^I{}_l(s)=(16\pi)^{-1}\int_{-1}^{+1}dZ\,P_l(Z)M^I(s,t)\,. \quad (3.20b)$$

Here Z is the cosine of the s-channel scattering angle in the center-of-mass system and the relative momentum in this system is

$$2k\equiv\{[s-(m_K+m_\pi)^2][s-(m_K-m_\pi)^2]/s\}^{1/2}.$$

The S- and P-wave amplitudes $A^{1/2}{}_0$, $A^{3/2}{}_0$, $A^{1/2}{}_1$, and $A^{3/2}{}_1$ may be computed from Eqs. (3.11), (3.19), and

(3.20). For the S-wave $I=\frac{1}{2}$ amplitude, we obtain

$$16\pi A^{1/2}{}_0=2\{Z_1+2(m_\pi{}^2+m_K{}^2)Z_3+4(m_\pi{}^2+m_K{}^2+k^2-s)Z_{10}+2k^2(Z_3-Z_2)\}$$

$$+3\left\{2Z_5\frac{1}{-s+m_\kappa{}^2}+Z_8+Z_7-(Z_8-Z_7)\frac{(m_K{}^2-m_\pi{}^2)^2}{(m_{K^*}{}^2)s}\right\}+2\left\{Z_4m_\sigma{}^{-2}[1-\tfrac{1}{2}x_\sigma L^{(0)}(x_\sigma)]\right.$$

$$+Z_5m_\kappa{}^{-2}L^{(2)}(x_\kappa)+Z_{11}m_\rho{}^{-2}[4(m_\pi{}^2+m_K{}^2-s)+(m_\rho{}^2+2s-2m_\pi{}^2-2m_K{}^2)x_\rho L^{(0)}(x_\rho)]-Z_8$$

$$\left.+\tfrac{1}{2}(Z_8-Z_7)m_{K^*}{}^{-2}\left(2m_\pi{}^2+2m_K{}^2-2s-m_{K^*}{}^2+\frac{(m_K{}^2-m_\pi{}^2)^2}{m_{K^*}{}^2}\right)L^{(2)}(x_{K^*})\right\}. \tag{3.21}$$

For the S-wave $I=\frac{3}{2}$ amplitude, we have

$$16\pi A^{3/2}{}_0=2\{Z_1+2(m_\pi{}^2+m_K{}^2)Z_3+2k^2(Z_3-Z_2)-2(m_\pi{}^2+m_K{}^2+k^2-s)Z_{10}\}$$
$$+\{2Z_4m_\sigma{}^{-2}[1-\tfrac{1}{2}x_\sigma L^{(0)}(x_\sigma)]-4Z_5m_\kappa{}^{-2}L^{(2)}(x_\kappa)-Z_{11}m_\rho{}^{-2}[4(m_\pi{}^2+m_K{}^2-s)+(m_\rho{}^2+2s-2m_\pi{}^2-2m_K{}^2)x_\rho L^{(0)}(x_\rho)]$$
$$+4Z_8-2(Z_8-Z_7)m_{K^*}{}^{-2}[2m_\pi{}^2+2m_K{}^2-2s-m_{K^*}{}^2+(m_K{}^2-m_\pi{}^2)^2/m_{K^*}{}^2]L^{(2)}(x_{K^*})\}, \tag{3.22}$$

where

$$x_a\equiv 4k^2/m_a{}^2,\quad \tfrac{1}{2}xL^{(0)}(x)=1-x^{-1}\ln(1+x),\quad\text{and}\quad x_aL^{(2)}(x_a)=\ln[(u_a+x_a')/(u_a+x_a'')],$$

with

$$x_a''=[s-(m_K+m_\pi)^2]/m_a{}^2,\quad x_a'\equiv x_a''-x_a,\quad\text{and}\quad u_a\equiv[m_a{}^2-(m_K-m_\pi)^2]/m_a{}^2.$$

In Eq. (3.21) the first curly bracket comes from the seagull diagrams, the second from the direct κ and K^* poles, and the third from the crossed-channel poles. In Eq. (3.22) the first curly bracket arises from the seagull diagrams and the second from the crossed-channel poles. No direct-channel poles are present since no $I=\frac{3}{2}$, $J=0$ meson appears to exist. The functions $L^{(2)}(x_a)$ have been constructed so that $L^{(2)}(0)=-1/u_a$. The $I=\frac{1}{2}$ P-wave amplitude is

$$12\pi k^{-2}A^{1/2}{}_1=\{Z_2-Z_3-2Z_{10}\}+\{Z_4m_\sigma{}^{-4}[1-L^{(1)}(x_\sigma)]+2Z_{11}m_\rho{}^{-4}(m_\rho{}^2+2s-2m_K{}^2-2m_\pi{}^2)$$
$$\times[+1-L^{(1)}(x_\rho)]-Z_5m_\kappa{}^{-4}L^{(3)}(x_\kappa)-\tfrac{1}{2}(Z_8-Z_7)m_{K^*}{}^{-4}[2m_K{}^2+2m_\pi{}^2-2s-m_{K^*}{}^2+(m_K{}^2-m_\pi{}^2)^2/m_{K^*}{}^2]L^{(3)}(x_{K^*})\}$$
$$+3(Z_8-Z_7)(-s+m_{K^*}{}^2)^{-1}. \tag{3.23}$$

For the $I=\frac{3}{2}$ P-wave amplitude we find

$$12\pi k^{-2}A^{3/2}{}_1=\{Z_2-Z_3+Z_{10}\}+\{Z_4m_\sigma{}^{-4}[1-L^{(1)}(x_\sigma)]-Z_{11}m_\rho{}^{-4}(m_\rho{}^2+2s-2m_K{}^2-2m_\pi{}^2)[1-L^{(1)}(x_\rho)]$$
$$+(Z_8-Z_7)m_{K^*}{}^{-4}[2m_K{}^2+2m_\pi{}^2-2s-m_{K^*}{}^2+(m_K{}^2-m_\pi{}^2)^2/m_{K^*}{}^2]L^{(3)}(x_{K^*})+2Z_5m_\kappa{}^{-4}L^{(3)}(x_\kappa)\}. \tag{3.24}$$

Here

$$xL^{(1)}(x)=x+12x^{-1}-6(x^{-1}+2x^{-2})\ln(1+x)$$

and

$$L^{(3)}(x_a)=12x_a{}^{-1}-6[x_a{}^{-1}+2(u_a+x_a'')x_a{}^{-2}]\ln[(u_a+x_a')/(u_a+x_a'')].$$

In Eq. (3.23) the first curly bracket arises from the seagull diagrams, the second curly bracket arises from the crossed-channel poles, and the third term comes from the direct-channel K^* pole. The first curly bracket in Eq. (3.24) comes from the seagull diagrams and the second from the crossed-channel poles. The functions $L^{(1)}(x_a)$ and $L^{(3)}(x_a)$ have the threshold values $L^{(1)}(0)=0$ and $L^{(3)}(0)=-1/u_a{}^2$.

C. Threshold Parameters

The scattering length $a^I{}_l$ and the effective range $r^I{}_l$ are defined by the threshold expansion

$$(m_\pi+m_K)k^{2l}\,\mathrm{Re}(A^I{}_l)^{-1}=(a^I{}_l)^{-1}+\tfrac{1}{2}r^I{}_lk^2+\cdots. \tag{3.25}$$

The S-wave scattering lengths[17] are obtained directly from Eqs. (3.21) and (3.22). Thus

$$8\pi(m_\pi+m_K)a^{1/2}{}_0=Z_1+(s_0+u_0)Z_3+Z_4m_\sigma{}^{-2}-2(s_0-u_0)(Z_{10}+Z_{11}m_\rho{}^{-2})$$
$$+Z_5\left(\frac{3}{-s_0+m_\kappa{}^2}+\frac{1}{-u_0+m_\kappa{}^2}\right)+(s_0-u_0-2m_K{}^2)(Z_8-Z_7)m_{K^*}{}^{-2}, \tag{3.26}$$

and

$$8\pi(m_\pi+m_K)a^{3/2}{}_0=Z_1+(s_0+u_0)Z_3+Z_4m_\sigma{}^{-2}+(s_0-u_0)(Z_{10}+Z_{11}m_\rho{}^{-2})$$
$$-2Z_5(-u_0+m_\kappa{}^2)^{-1}-\tfrac{1}{2}(s_0-u_0+4m_K{}^2)(Z_8-Z_7)m_{K^*}{}^{-2}, \tag{3.27}$$

[17] Hard-meson S-wave scattering lengths have also been obtained by L. K. Pande (private communication).

where the threshold values of the invariants s and u are $s_0=(m_K+m_\pi)^2$ and $u_0=(m_K-m_\pi)^2$, respectively. The effective ranges are

$$
\begin{aligned}
&-8\pi(m_\pi+m_K)(a^{1/2}{}_0)^2 r^{1/2}{}_0 \\
&\quad=4(Z_3-Z_2)-4Z_4 m_\sigma^{-4}+32Z_{11}\frac{m_\pi m_K}{m_\rho^4}+\frac{1}{m_\pi m_K}\biggl\{Z_5\biggl(\frac{6s_0}{(-s_0+m_\kappa^2)^2}+\frac{s_0+u_0}{(-u+m_\kappa^2)^2}\biggr) \\
&\qquad+8(m_\pi m_K-s_0)(Z_{10}+Z_{11}m_\rho^{-2})+(Z_8-Z_7)\biggl[\frac{-3u_0}{m_{K^*}^2}+\frac{1}{-u_0+m_{K^*}^2}\biggl(2s_0-\frac{(s_0+u_0)(s_0+m_{K^*}^2)}{2m_{K^*}^2}\biggr)\biggr]\biggr\}, \qquad (3.28)
\end{aligned}
$$

$$
\begin{aligned}
&-8\pi(m_\pi+m_K)(a^{3/2}{}_0)^2 r^{3/2}{}_0 \\
&\quad=4(Z_3-Z_2)-4Z_4 m_\sigma^{-4}-16Z_{11}\frac{m_\pi m_K}{m_\rho^4}-\frac{2}{m_\pi m_K}\biggl\{Z_5\frac{s_0+u_0}{(-u_0+m_\kappa^2)^2}+2(m_\pi m_K-s_0)(Z_{10}+Z_{11}m_\rho^{-2}) \\
&\qquad+(Z_8-Z_7)\frac{1}{-u_0+m_{K^*}^2}\biggl[2s_0-\frac{(u_0+s_0)(s_0+m_{K^*}^2)}{2m_{K^*}^2}\biggr]\biggr\}. \qquad (3.29)
\end{aligned}
$$

The soft-pion analysis of Weinberg[18] predicts the S-wave scattering lengths to be

$$
\begin{aligned}
a^{1/2}{}_0&=2L(1+m_\pi/m_K)^{-1}=0.130m_\pi^{-1}, \\
a^{3/2}{}_0&=-L(1+m_\pi/m_K)^{-1}=-0.065m_\pi^{-1},
\end{aligned}
\qquad (3.30)
$$

where $L=(m_\pi/8\pi F_\pi^2)=0.0825m_\pi^{-1}$. To compare these results with our hard-meson calculation, the scattering lengths are computed for three representative values of F_K/F_π. The results are displayed in Table I. The $I=\frac{1}{2}$ S-wave scattering lengths are insensitive to the value of F_K/F_π and differ from the soft-meson value by 10–15%. On the other hand, the $I=\frac{3}{2}$ scattering lengths change rapidly with the ratio F_K/F_π and correct the soft-meson values by as much as 40%. Both $A^{1/2}{}_0$ and $A^{3/2}{}_0$ contain terms which behave like $\alpha m_\kappa^2/m_K^2$ and $\alpha m_\kappa^2/m_\pi^2$. These terms represent the "nongentle" behavior created by the current algebra conditions. Thus, the hard-meson corrections are rather modest considering the size of some of the terms in the $K\pi$ amplitude. In applying the Veneziano model to $K\pi$ scattering, Lovelace[19] finds that the S-wave scattering lengths have the values $a^{1/2}{}_0=0.215\ m_\pi^{-1}$ and $a^{3/2}{}_0=-0.097\ m_\pi^{-1}$. This result deviates from the soft-pion values considerably.

TABLE I. Hard-meson S-wave $K\pi$ scattering lengths for the $I=\frac{1}{2}$, $\frac{3}{2}$ channels in units of m_π^{-1}.

Hard-meson scattering lengths in $(m_\pi)^{-1}$ \ F_K/F_π	1.169	1.190	1.220
$a^{1/2}{}_0$	+0.115	+0.117	+0.112
$a^{3/2}{}_0$	−0.090	−0.072	−0.049

[18] S. Weinberg, Phys. Rev. Letters **17**, 616 (1966).
[19] C. Lovelace, in Ref. 1.

Next we use Eqs. (3.28) and (3.29) to compute the hard-meson S-wave effective ranges. The results are recorded in Table II.

It is interesting to notice that the expansion (3.25) has an S-wave spurious zero at about 100 MeV above threshold. Thus, this effective range expansion is valid in only a small region about threshold. However, the expansion

$$A^I{}_0=(m_\pi+m_K)[a^I{}_0-\tfrac{1}{2}(a^I{}_0)^2 r^I{}_0 k^2+\cdots] \qquad (3.31)$$

is reasonably convergent in the low-energy region. In fact, Eq. (3.31) represents a good approximation (to within 15%) to the full S-wave amplitude for $\sqrt{s}\lesssim 900$ MeV.

Next we discuss the P-wave scattering lengths and effective ranges. Using Eqs. (3.23) and (3.24) in the expansion (3.25), the P-wave scattering lengths are

TABLE II. Hard-meson S-wave $K\pi$ effective ranges for $I=\frac{1}{2}$, $\frac{3}{2}$ in units of m_π^{-1}.

Hard-meson effective ranges in $(m)_\pi^{-1}$ \ F_K/F_π	1.169	1.190	1.220
$r^{1/2}{}_0$	−12.0	−10.6	−11.0
$r^{3/2}{}_0$	+14.2	+20.9	+39.6

TABLE III. Hard-meson P-wave $K\pi$ scattering lengths (in units of m_π^{-3}) and effective ranges (in units of m_π) for the $I=\frac{1}{2}$, $\frac{3}{2}$ channels.

P-wave threshold parameters \ F_K/F_π	1.169	1.190	1.220
$a^{1/2}{}_1$ (m_π^{-3})	15.3×10^{-3}	15.0×10^{-3}	14.1×10^{-3}
$a^{3/2}{}_1$ (m_π^{-3})	5.0×10^{-3}	12.0×10^{-3}	24.0×10^{-3}
$r^{1/2}{}_1$ (m_π)	−35.5	−36.6	−46.8
$r^{3/2}{}_1$ (m_π)	−350	−48.6	−81.3

determined to be

$$12\pi(m_\pi+m_K)a^{1/2}{}_1=Z_2-Z_3+Z_4m_\sigma^{-4}-2(Z_{10}+m_\rho^{-2}Z_{11})-2\frac{s_0-u_0}{m_\rho^4}Z_{11}+(Z_8-Z_7)\left[\frac{3}{-s_0+m_{K^*}^2}-\left(\frac{1}{2m_{K^*}^2}\right)\frac{s_0+m_{K^*}^2}{-u_0+m_{K^*}^2}\right]+\frac{Z_5}{-u_0+m_\kappa^2},\quad(3.32)$$

$$12\pi(m_\pi+m_K)a^{3/2}{}_1=Z_2-Z_3+Z_4m_\sigma^{-4}+(Z_{10}+m_\rho^{-2}Z_{11})+\frac{s_0-u_0}{m_\rho^4}Z_{11}+(Z_8-Z_7)m_{K^*}^{-2}\frac{s_0+m_{K^*}^2}{-u_0+m_{K^*}^2}-2Z_5\frac{1}{-u_0+m_\kappa^2},\quad(3.33)$$

and the effective ranges are

$$-(m_\pi+m_K)3\pi(a^{1/2}{}_1)^2r^{1/2}{}_1$$
$$=-2Z_4m_\sigma^{-6}-4Z_{11}\frac{u_0-s_0-m_\rho^2}{m_\rho^6}-2\frac{s_0}{m_\pi m_K}Z_{11}m_\rho^{-4}+(Z_8-Z_7)\frac{s_0}{m_\pi m_K}\left[\frac{3}{(-s_0+m_{K^*}^2)^2}-\frac{1}{(-u_0+m_{K^*}^2)^2}\right]-(Z_8-Z_7)m_{K^*}^{-4}\frac{s_0+m_{K^*}^2}{-u_0+m_{K^*}^2}R_{K^*}+2Z_5m_\kappa^{-2}\frac{1}{(-u+m_\kappa^2)^2}R_\kappa,\quad(3.34)$$

$$-(m_\pi+m_K)3\pi(a^{3/2}{}_1)^2r^{3/2}{}_1$$
$$=-2Z_4m_\sigma^{-6}+2Z_{11}\frac{u_0-s_0-m_\rho^2}{m_\rho^6}+\frac{s_0}{m_\pi m_K}Z_{11}m_\rho^{-4}+(Z_8-Z_7)\frac{s_0}{m_\pi m_K}\frac{1}{(-u_0+m_{K^*}^2)^2}+2(Z_8-Z_7)m_{K^*}^{-4}\frac{s_0+m_{K^*}^2}{-u_0+m_{K^*}^2}R_{K^*}-4Z_5m_\kappa^{-2}\frac{1}{(-u_0+m_\kappa^2)^2}R_\kappa,\quad(3.35)$$

where

$$R_a\equiv(16m_\pi^2m_K^2)^{-1}\left[(s_0+u_0)^2+\frac{s_0^2+2u_0s_0-u_0^2}{m_a^2-u_0}m_a^2\right].$$

The values of the P-wave threshold parameters obtained from Eqs. (3.32)–(3.35) are shown in Table III with the appropriate units given in parentheses.

As was the case for S waves, the P wave parameters also exhibit the sensitivity of the $I=\frac{3}{2}$ quantities to the ratio F_K/F_π.

IV. COMPARISON WITH EXPERIMENT

In this section, the hard-meson phase shifts and cross sections are compared with experiment. Later in the section a comparison with the predictions of the Lovelace-Veneziano model is also made.

1. S wave. As previously indicated, the expansion equation (3.31) may be used as a good approximation to the full $I=\frac{1}{2}$ amplitude equation (3.21) for $\sqrt{s}\lesssim 900$ MeV. However, as we approach the κ resonance it becomes necessary to use the full amplitude of Eq. (3.21). In this region the $I=\frac{1}{2}$ channel is dominated by the κ pole with the threshold parameters $a^{1/2}{}_0$, $r^{1/2}{}_0$, making negligible contributions and the amplitude is effectively controlled by the parameters F_K/F_π and m_κ^2 (and hence the κ width). In order to extract the phase shifts from the current-algebra amplitudes, we proceed by imposing two-body unitarity on each partial-wave amplitude separately. We assume that Eqs. (3.21) and (3.22) correctly determine $\mathrm{Re}(A^I{}_0)^{-1}$ but not $\mathrm{Im}(A^I{}_0)^{-1}$. Unitarity is restored by replacing $ks^{-1/2}A^I{}_0$ by $\tan\delta^I{}_0$ in these equations.[4] Theoretical curves obtained from the unitarized S-wave current-algebra amplitudes are displayed in Fig. 1 for the representative values F_K/F_π

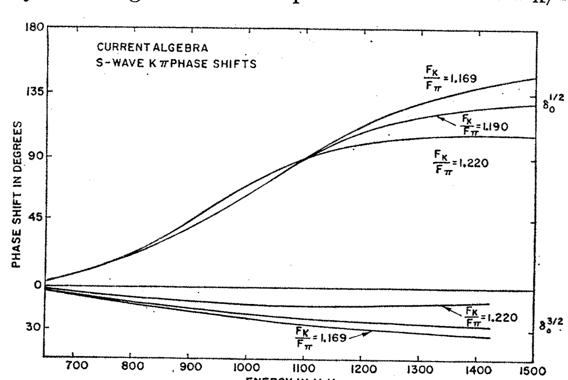

FIG. 1. Current-algebra curves for the S-wave phase shifts ($I=\frac{1}{2}$ upper curves, $I=\frac{3}{2}$ lower curves) with $m_\kappa=1100$ MeV.

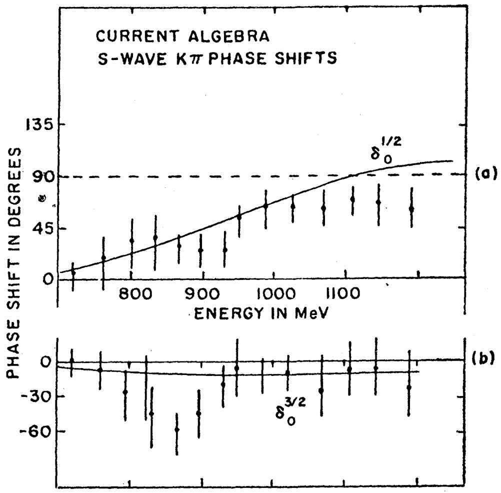

FIG. 2. S-wave phase shifts with $m_\kappa=1100$ MeV and $F_K/F_\pi=1.220$. (a) $I=\frac{1}{2}$ channel; the experimental points are the Mercer *et al.* down-down solution (Ref. 20). (b) $I=\frac{3}{2}$ channel; the experimental points are the Mercer *et al.* down-up solution (Ref. 20).

$=1.169$, 1.190, and 1.220. These values of F_K/F_π correspond to a κ width $\Gamma(\kappa\rightarrow K\pi)\cong 450$, 525, and 850 MeV, respectively, for κ mass $m_\kappa=1100$ MeV of Trippe *et al.*[14] The condition (2.27d) establishes 450 MeV as the minimum allowed width for this κ meson in good agreement with the experimental estimate of $\Gamma(\kappa\rightarrow K\pi)\cong 400$ MeV of Trippe *et al.*[14] Contrary to Trippe *et al.*, however, a non-negligible $I=\frac{3}{2}$ interaction is predicted. The $I=\frac{3}{2}$ phase shifts are seen to be sensitive to the ratio F_K/F_π over the entire energy range. The $I=\frac{1}{2}$ phase shifts are insensitive to the value of F_K/F_π in the threshold region and vary by less than 15% in the region below the κ mass. Above this energy region, the theoretical curves are governed solely by the parameter

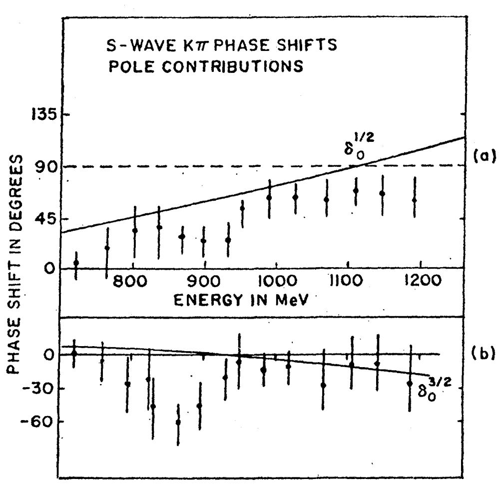

FIG. 3. S-wave phase shifts obtained from direct-channel and crossed-channel poles only. $F_K/F_\pi=1.220$ and $m_\kappa=1100$ MeV. The experimental points are from Mercer *et al.* (Ref. 20). (a) $I=\frac{1}{2}$ channel; the data points are the down-down solution. (b) $I=\frac{3}{2}$ channel; the data are the down-up solution (Ref. 20).

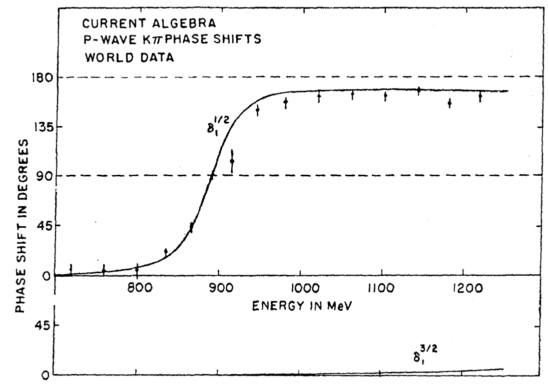

FIG. 4. P-wave phase shifts (upper curve for $I=\frac{1}{2}$, lower curve for $I=\frac{3}{2}$). The experimental points are from Mercer *et al.* (Ref. 20); $F_K/F_\pi=1.220$.

F_K/F_π. Thus with good phase-shift data an accurate experimental determination of this ratio is feasible.

Next we consider the experimental analysis of Mercer *et al.*[20,21] This analysis implies that the $I=\frac{1}{2}$ S-wave phase shift rises slowly toward 90° in the 900–1200 MeV region and that the corresponding $I=\frac{3}{2}$ phase shift is negative and generally small over the entire energy domain. The $I=\frac{1}{2}$ interaction is examined in Fig. 2(a), the experimental points being the "down-down" solution.[22] We exhibit the current-algebra fit to these data for $F_K/F_\pi=1.220$ and $m_\kappa=1100$ MeV. The theoretical curve follows the general trend of the experimental points, but it does not produce the dip at 900 MeV and overshoots the data above 1050 MeV. These results appear to be consistent[20] with a broad resonance at the mass of Trippe *et al.* with a width of 850 MeV. In Fig. 2(b), the $I=\frac{3}{2}$ phase shift is shown, the

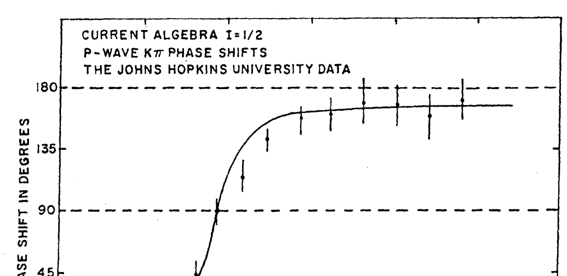

FIG. 5. $I=\frac{1}{2}$ P-wave phase shift with $F_K/F_\pi=1.220$. The experimental points are from Mercer *et al.* (Ref. 20).

[20] R. Mercer, P. Antich, A. Callahan, C.-Y. Chien, B. Cox, R. Carson, D. Denegri, L. Ettlinger, D. Feiock, G. Goodman, J. Haynes, A. Pevsner, R. Sekulin, V. Sreendhar, and R. Zdanis, The Johns Hopkins University report (unpublished).

[21] It is worth noting that the analysis of Ref. 20 does not *a priori* assume a negligible S-wave $I=\frac{3}{2}$ interaction as is done in many other analyses (see, e.g., Refs. 14 and 1).

[22] A number of solutions exist for the S-wave phase-shift analysis Ref. 20. Of these, the $I=\frac{1}{2}$ down-down and the $I=\frac{3}{2}$ down-up solutions lead to total cross sections which best represent the cross section obtained by extrapolation.

experimental points being the "down-up" solution of Mercer *et al.*[20] The theoretical curve is that for $F_K/F_\pi=1.220$.

The amplitudes of Eqs. (3.21) and (3.22) contain a set of terms which are characteristic of the current algebra solution, namely, the seagull terms. These terms generally tend to cancel the crossed-pole contributions to the S-wave amplitudes. This behavior is illustrated by considering an amplitude composed of only direct- and crossed-channel poles:

$$\begin{aligned}16\pi A^{1/2}{}_0' = {} & 6Z_5(-s+m_\kappa^2)^{-1}+2\{Z_5 m_\kappa^{-2}L^{(2)}(x_\kappa)\\ & +Z_4 m_\sigma^{-2}x_\sigma^{-1}\ln(1+x_\sigma)-Z_8\\ & +\tfrac{1}{2}(Z_8-Z_7)m_{K^*}^{-2}(s_0+u_0-2s-m_{K^*}^2\\ & +s_0u_0/m_{K^*}^2)L^{(2)}(x_{K^*})+2Z_{11}m_\rho^{-2}[s_0+u_0\\ & -2s+\tfrac{1}{2}(m_\rho^2+2s-s_0-u_0)x_\rho L^{(0)}(x_\rho)]\}\,,\end{aligned}\tag{4.1}$$

$$\begin{aligned}16\pi A^{3/2}{}_0' = {} & -4Z_5 m_\kappa^{-2}L^{(2)}(x_\kappa)+2Z_4 m_\sigma^{-2}x_\sigma^{-1}\ln(1+x_\sigma)\\ & +4Z_8-2(Z_8-Z_7)m_{K^*}^{-2}(s_0+u_0-2s-m_{K^*}^2\\ & +s_0u_0/m_{K^*}^2)L^{(2)}(x_{K^*})-2Z_{11}m_\rho^{-2}[s_0+u_0-2s\\ & +\tfrac{1}{2}(m_\rho^2+2s-s_0-u_0)x_\rho L^{(0)}(x_\rho)].\end{aligned}\tag{4.2}$$

These amplitudes do not satisfy the current-algebra constraints since the seagull parts are needed for that purpose. The agreement with the data is drastically changed as shown in Fig. 3. The theoretical curves exhibit significantly larger phase shifts in the low-energy and high-energy regions, thus illustrating the cancellations that occur between the seagull and crossed-pole pieces of the current-algebra amplitudes.

2. P wave. The extraction of the P-wave phase shifts is accomplished by unitarizing the current-algebra amplitudes in analogy with the S-wave case. Thus, in Eqs. (3.23) and (3.24) $ks^{-1/2}A^I{}_1$ is replaced by $\tan\delta^I{}_1$. The $I=\frac{1}{2}$ phase shift is compared with the experimental data of Mercer *et al.*[20] This analysis presumes that the $I=\frac{3}{2}$ P-wave interaction is negligible, in accordance with the current-algebra prediction shown in Fig. 4. A good theoretical fit to the $I=\frac{1}{2}$ experimental points shown in Figs. 4 and 5 can be obtained for $F_K/F_\pi=1.220$. The current-algebra phase shifts are essentially independent of F_K/F_π below 1000 MeV.

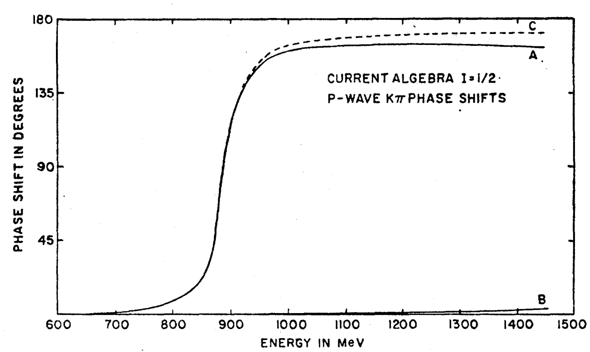

FIG. 6. $I=\frac{1}{2}$ P-wave phase shift. $F_K/F_\pi=1.220$. Curve A is the total theoretical amplitude. Curve B is the total amplitude with the direct K^* pole deleted. Curve C is the amplitude obtained from direct-channel and crossed-channel poles only.

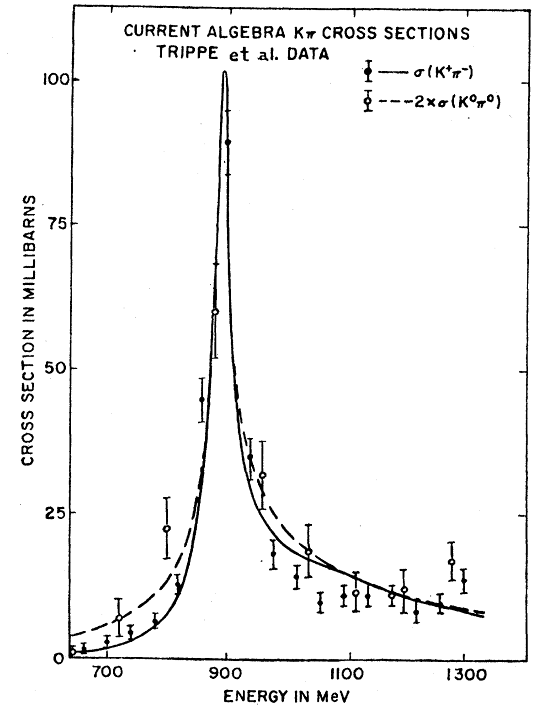

FIG. 7. Total $K\pi$ cross sections. $F_K/F_\pi=1.220$. The solid curve represents the current-algebra results for the elastic cross section and the dashed curve corresponds to twice the charge-exchange cross section. The experimental points (black dots for elastic and white dots for twice charge exchange) are those of Trippe *et al.* (Ref. 14) obtained from the reaction $K^+p\to K\pi\Delta^{++}$.

The unitarized $I=\frac{1}{2}$ P-wave amplitude is well approximated by a simple direct-channel K^* pole. This behavior is illustrated in Fig. 6 where curve A represents the full theoretical amplitude, and curve B represents that amplitude with the direct K^* pole deleted. For the $I=\frac{1}{2}$ S-wave amplitude, it was shown that the seagull and crossed-channel poles mostly canceled each other both in the threshold region and in the region past the κ pole. In the P-wave case, the seagull and crossed-channel terms are individually small over the entire energy range under consideration, yet they have a tendency to cancel. Thus the direct K^* pole completely

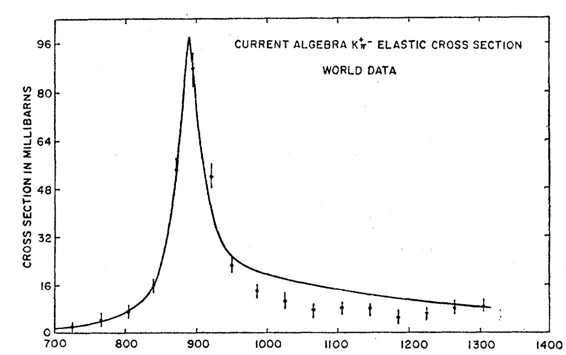

FIG. 8. Total elastic $K^+\pi^-$ cross section. $F_K/F_\pi=1.220$ and $m_\kappa=1100$ MeV. The experimental points are from Mercer *et al.* (Ref. 20) for the reaction $K^+p\to K^+\pi^-\Delta^{++}$.

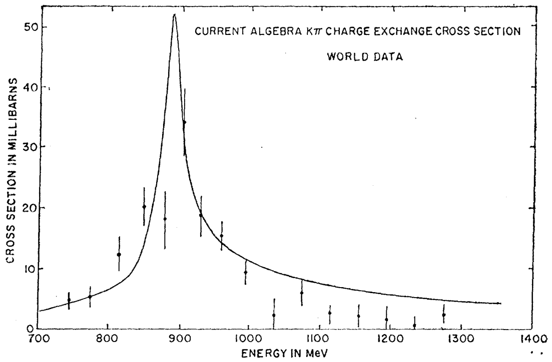

FIG. 9. Total charge-exchange $K\pi$ cross section. $F_K/F_\pi=1.220$ and $m_\kappa=1100$ MeV. The experimental points are from Ref. 20 for the reaction $K^+p\to K^0\pi^0\Delta^{++}$.

dominates the full amplitude. If the seagull parts are deleted, we obtain for the P-wave amplitude in the $I=\frac{1}{2}$ channel

$$\begin{aligned}12\pi k^{-2}A^{1/2}{}_1{}' = &+3(Z_8-Z_7)(-s+m_{K^*}{}^2)^{-1}\\ &-Z_5 m_\kappa{}^{-4}L^{(3)}(x_\kappa)-Z_4 m_\sigma{}^{-4}[1-L^{(1)}(x_\sigma)]\\ &+2Z_{11}m_\rho{}^{-4}(s_0+u_0-2s-m_\rho{}^2)[1-L^{(1)}(x_\rho)]\\ &-\tfrac{1}{2}(Z_8-Z_7)m_{K^*}{}^{-4}(s_0+u_0-m_{K^*}{}^2-2s+u_0s_0/m_{K^*}{}^2)\\ &\times[L^{(3)}(x_{K^*})]. \quad (4.3)\end{aligned}$$

The predictions obtained by unitarizing this amplitude are presented as curve C of Fig. 6. There is no significant deviation from the full P-wave current-algebra amplitude. Experimentally, the $I=\frac{1}{2}$ P-wave amplitude is well represented by a Breit-Wigner form over the entire energy range. Thus we find excellent agreement between the current algebra and experiment for this case.

3. Elastic and charge-exchange cross sections. Next we consider the elastic and charge-exchange cross sections predicted by current algebra. In the region of validity of the present calculation, only the S and P waves are important and the D and higher partial waves are negligible. First we consider the experimental data of Trippe *et al.*[14] Hard-meson cross sections are given in Fig. 7. The solid curve should coincide with the black points and the dashed curve with the white points. This experimental analysis supposes that the $I=\frac{3}{2}$ interaction is negligible. The current-algebra curves are in good agreement with the data through the K^* resonance and are insensitive to the parameter F_K/F_π in this region. Above this energy region, the theoretical curves are consistent with the data, although they do not reproduce the dip at $\simeq$1050 MeV.

Next, the experimental cross sections of Mercer *et al.*[20] are examined. A current-algebra curve with $F_K/F_\pi=1.220$ is fitted to the $K^+\pi^-\to K^+\pi^-$ data as shown in

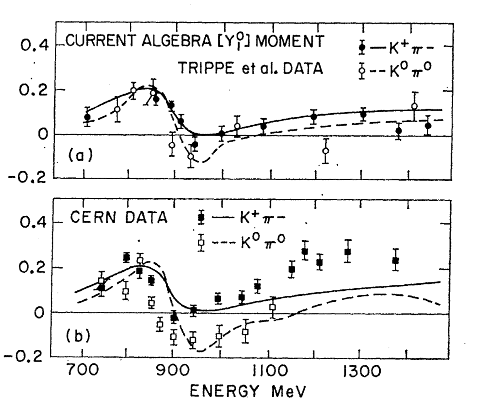

FIG. 10. The current-algebra $\langle Y_1{}^0\rangle$ moment for $K^+\pi^-$ elastic (solid curves and black points) and charge-exchange (dashed curves and white points) processes. $m_\kappa=1100$ MeV. (a) $F_K/F_\pi=1.220$; experimental points are from Ref. 14. (b) $F_K/F_\pi=1.169$; experimental points are those of Ref. 24.

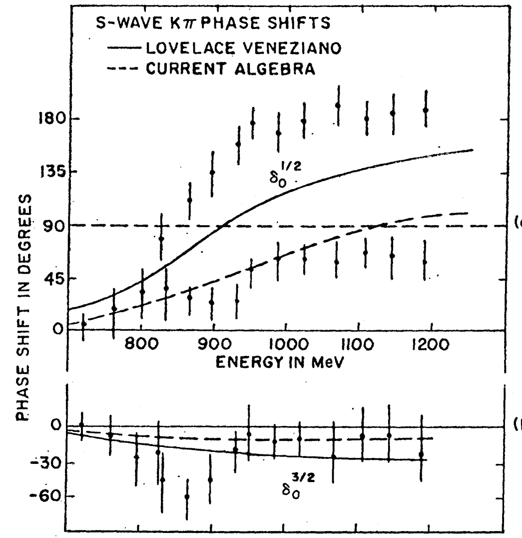

FIG. 11. Veneziano S-wave $K\pi$ phase shifts (solid curves) from Lovelace (Ref. 19). (a) $I=\frac{1}{2}$ channel; experimental points are the down-down (lower set above 800 MeV) and the down-up (upper set above 800 MeV) solutions of Mercer *et al.* (Ref. 20). (b) $I=\frac{3}{2}$ channel; experimental points are the down-up of Ref. 20. The dashed curves represent the current-algebra phase shifts of Fig. 2.

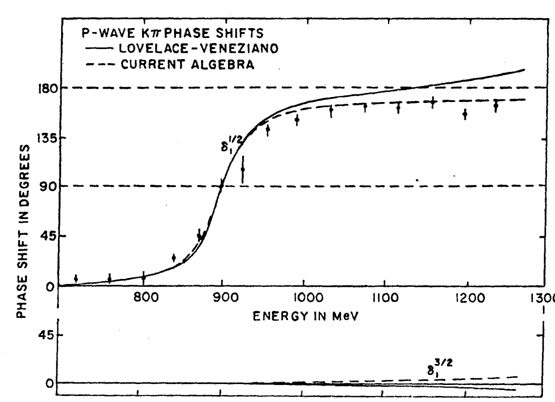

FIG. 12. Veneziano P-wave $K\pi$ phase shifts (solid curves) from Ref. 19. The experimental points are from Ref. 20. The current-algebra phase shifts (dashed curves) have $F_K/F_\pi=1.220$ and $m_\kappa=1100$ MeV.

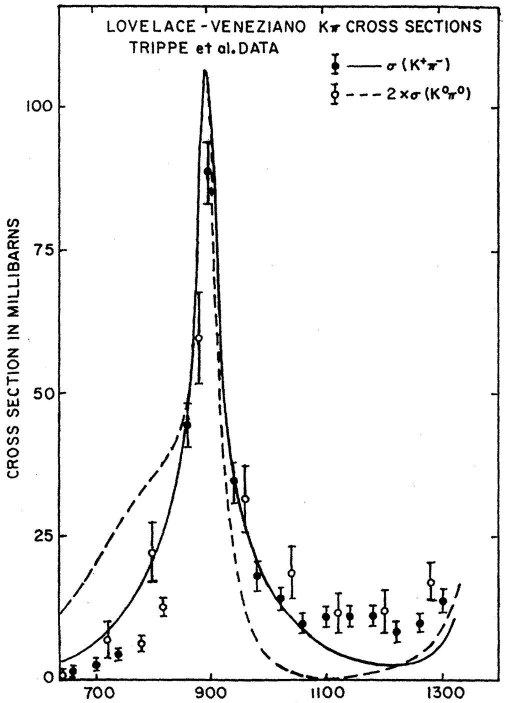

FIG. 13. Total Veneziano cross sections from Lovelace (Ref. 19). The solid curves represent the elastic cross section and the dashed curves represent twice the charge-exchange cross section. The experimental points are from Trippe *et al.* (Ref. 14).

Fig. 8. Excellent agreement with the experimental elastic cross section is obtained through the K^* region. However, the theoretical curve passes above the data in the 1000–1200-MeV region. In Fig. 9 the experimental points for the charge-exchange cross section for $K^+\pi^- \to K^0\pi^0$ are given. Again the theoretical curve has $F_\kappa/F_\pi = 1.220$. Reasonable agreement with experiment is attained up to the κ mass, above which the theoretical

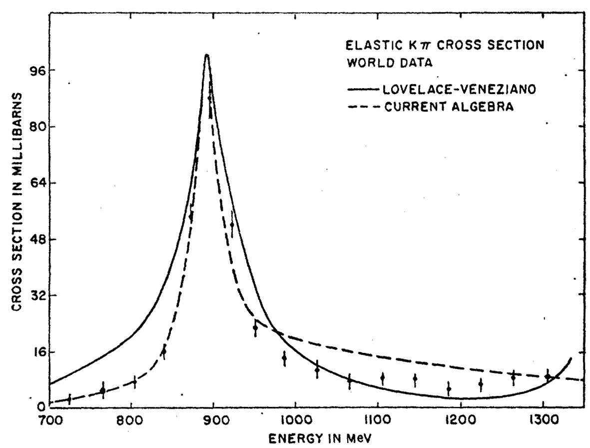

FIG. 14. The Lovelace-Veneziano elastic cross section (solid curve). The experimental points are from Mercer *et al.* (Ref. 20). The dashed curve represents the current-algebra prediction shown in Fig. 8.

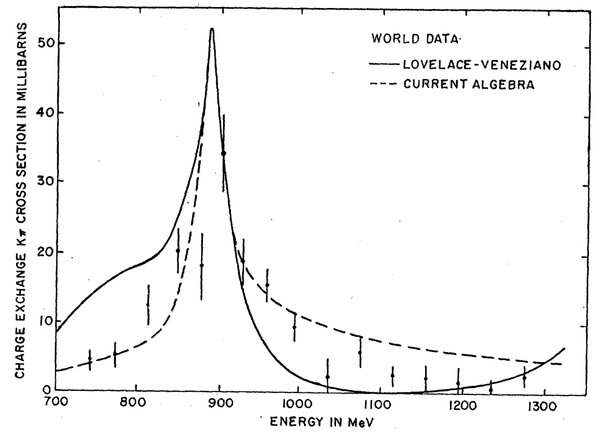

FIG. 15. The Lovelace-Veneziano charge-exchange cross section (solid curve). The experimental data are from Ref. 20. The dashed curve represents the current-algebra results of Fig. 9.

curve lies somewhat higher than the experimental points.

4. Moment $\langle Y_1^0\rangle$. It is interesting to consider the $\langle Y_1^0\rangle$ moment in the angular distribution for the $K^+\pi^-$ elastic and charge-exchange processes. The moment is defined by

$$\langle Y_1^0\rangle \propto \mathrm{Re}(A_S A_P^*)/(|A_S|^2+3|A_P|^2), \qquad (4.4)$$

where $A_S=\frac{1}{3}(2A^{1/2}{}_0+A^{3/2}{}_0)$ for the elastic process, and $A_S=\frac{1}{3}\sqrt{2}(-A^{1/2}{}_0+A^{3/2}{}_0)$ for the charge-exchange process. The S-wave amplitudes $A^{1/2}{}_0$, $A^{3/2}{}_0$ have been defined in Eqs. (3.21) and (3.22). A_P is similarly constructed using the P-wave amplitudes of Eqs. (3.23) and (3.24). The current-algebra $\langle Y_1^0\rangle$ moment for $K^+\pi^- \to K^-\pi^-$ is independent of F_K/F_π throughout most of the energy range under consideration. On the other hand, for $K^+\pi^- \to K^0\pi^0$ the moment is independent of F_K/F_π only through the K^* region. Above this energy region the angular distribution is very sensitive to F_K/F_π. The hard-meson $\langle Y_1^0\rangle$ moment is compared with the experimental data in Fig. 10.[23] The solid curves correspond to the black points and the dashed curves correspond to the white points. The theoretical curve having $F_K/F_\pi=1.220$ is in good agreement with the analysis of Trippe *et al.*,[14] as shown in Fig. 10(a). In Fig. 10(b), the current-algebra curve $F_K/F_\pi=1.169$ is compared to the CERN analysis[24] (at higher energies there is some discrepancy with the preceding analysis). Clearly a significant success of the current-algebra results in the moment analysis is the prediction of the dip above 900 MeV for the charge-exchange reaction and not for the elastic reaction, as confirmed by experiment.

5. Comparison with the Lovelace-Veneziano model. We wish to compare the hard-meson current-algebra

[23] The hard-meson moment $\langle Y_1^0\rangle$ for the elastic process has been normalized at 810 MeV to the data of Ref. 14.

[24] CERN, private communication, as cited by C. Lovelace, in Ref. 1.

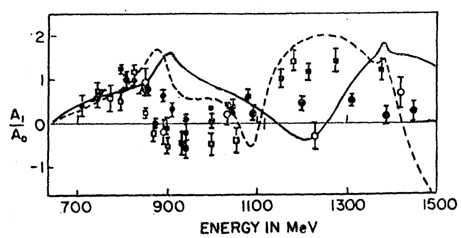

FIG. 16. The Lovelace-Veneziano $\langle Y_1{}^0\rangle$ moment from Ref. 19. The solid curve and black dots represent the elastic $K^+\pi^-$ moment, and the dashed curve (and white dots) represents the charge exchange $K^+\pi^-$ moment. The circular experimental points are from Trippe *et al.* (Ref. 14) and the square ones from CERN (Ref. 24).

results with the recent work of Lovelace,[19] who has used the Veneziano formula to analyze $K\pi$ scattering. In Fig. 11, the S-wave Lovelace-Veneziano results are compared with the experimental analysis of Mercer *et al.*[20] and the current-algebra results. The experimental points for the $I=\frac{1}{2}$ channel correspond to the down-down (lower) and down-up (upper) solutions, The Lovelace-Veneziano model predicts a broad resonance in this channel at about 900 MeV as opposed to that of Trippe *et al.*[14] at 1100 MeV. Referring to Fig. 11, we find that the Lovelace-Veneziano model in this channel differs considerably from the current-algebra result and is a poor fit to the experiment over the entire energy domain. We note that the down-down points are the favored solution in this channel.[20] On the other hand, the Lovelace-Veneziano model gives an S-wave phase shift which is consistent with experiment [see Fig. 11(b)] for $I=\frac{3}{2}$ scattering. In Fig. 12, the Lovelace-Veneziano P-wave phase shifts are compared with the data of Ref. 20 and the current-algebra results. Here the $I=\frac{1}{2}$ prediction is in good agreement with these other results up to 1000 MeV. However, the Lovelace-Veneziano phase shift in this channel passes through 180° at 1100 MeV. There appears to be no experimental evidence to substantiate this behavior.[20] On the other hand, both the current-algebra and the Lovelace-Veneziano model predict negligible interactions in the P-wave $I=\frac{3}{2}$ channel, in agreement with experiment.

The Lovelace-Veneziano cross sections for the elastic $K^+\pi^- \to K^+\pi^-$ and charge-exchange $K^+\pi^- \to K^0\pi^0$ processes are plotted against the experimental points[19,20] in Figs. 13–15. The model exhibits poor threshold behavior, while the hard-meson cross sections are in good agreement with experiment in this region. On the other hand, the cross sections of the Lovelace-Veneziano model are in somewhat better agreement with the experimental data above the 1000-MeV region. Finally, the lovelace-Veneziano predictions for $\langle Y_1{}^0\rangle$ are shown in Fig. 16 and are seen to be a poor fit to the data.[19] In particular, this model does not produce a dip around 900 MeV for the charge-exchange reaction, conflicting with current algebra and experiment.

In conclusion, we remark that the hard-meson current-algebra results are in excellent agreement with experiment below the 1000–1100-MeV region. Above this energy region, one must take into consideration other channels like $K\eta$ which become physical for a more quantitative comparison with experiment.

ACKNOWLEDGMENT

It is with great pleasure and appreciation that the author thanks Professor Pran Nath for his guidance and for many stimulating and informative discussions during the course of this work.